Quantitative and Qualitative Involvement of P3N-PIPO in Overcoming Recessive Resistance against *Clover yellow vein virus* in Pea Carrying *cyv1*

Sun Hee Choi, Yuka Hagiwara-Komoda, Kenji S Nakahara[#], Go Atsumi, Ryoko Shimada, Yusuke Hisa, Satoshi Naito, Ichiro Uyeda[#]

Division of Applied Bioscience, Graduate School of Agriculture, Hokkaido University, Sapporo 060-8589

Running title: Role of P3N-PIPO in ClYVV virulence against *cyv1* pea

Corresponding authors: I. Uyeda, E-mail: uyeda@res.agr.hokudai.ac.jp; K.S. Nakahara, E-mail: knakahar@res.agr.hokudai.ac.jp

Phone: +81 11 706 2490

Fax: +81 11 706 2483

Abstract

In pea carrying *cyv1*, a recessive gene for resistance to *Clover yellow vein virus* (ClYVV), ClYVV isolate Cl-no30 was restricted to the initially infected cells whereas isolate 90-1 Br2 overcame this resistance. We mapped the region responsible for breaking of *cyv1*-mediated resistance by examining infection of *cyv1* peas with chimeric viruses constructed from parts of Cl-no30 and 90-1 Br2. The breaking of resistance was attributed to the P3 cistron, which is known to produce two proteins: P3, from the main open reading frame (ORF), and P3N-PIPO, which has the N-terminal part of P3 fused to amino acids encoded by a small ORF (called PIPO) in the +2 reading frame. We introduced point mutations that were synonymous with respect to the P3 protein but non-synonymous with respect to the P3N-PIPO protein, and vice versa, into the chimeric viruses. Infecting plants with these mutant viruses revealed that both P3 and P3N-PIPO were involved in overcoming *cyv1*-mediated resistance. Moreover, P3N-PIPO quantitatively affected the virulence of Cl-no30 in *cyv1* peas. Additional expression in *trans* of the P3N-PIPO derived from Cl-no30, using *White clover mosaic virus* as a vector, enabled Cl-no30 to move to systemic leaves in *cyv1* peas. Susceptible pea plants infected with chimeric ClYVV possessing the P3 cistron of 90-1 Br2, and which were therefore virulent toward *cyv1* peas, accumulated more P3N-PIPO than did those infected with Cl-no30, suggesting that the higher level of P3N-PIPO in infected cells contributed to the breaking of resistance by 90-1 Br2. This is the first report showing that P3N-PIPO is a virulence determinant in plants resistant to a potyvirus.

Introduction

Breeding by transfer of natural resistance genes between varieties of crops and from wild ancestors into crops is one of the major strategies to confer resistance against viruses and other pathogens. However, pathogen mutants that overcome the resistance seem to inevitably emerge. Understanding how pathogens overcome host plant resistance is important for developing strategies to confer durable resistance to crops.

Plant resistance against viruses, and especially potyviruses, frequently shows recessive inheritance (1). Most of the recessive resistance genes in crops have been identified as *eukaryotic initiation factors* (*eIFs*), such as the *eIF4E* and *eIF4G* families of genes that control potyviruses (2). In particular, the recessive resistance genes *cyv2* (resistance to *Clover yellow vein virus* [ClYVV]); *sbm-1*, *-3*, and *-4* (resistance to *Pea seed-borne mosaic virus* [PSbMV]); *wlv* (resistance to *Bean yellow mosaic virus* [BYMV]), in pea (*Pisum sativum*); and $mo1^1$ and $mo1^2$ (resistant to *Lettuce mosaic virus* [LMV]) have been identified as identical or allelic genes that encode eIF4E (3-5). eIF4E interacts with the potyviral genome–linked protein VPg at the surface, near a cap-binding pocket (5-10). However, the eIF4Es derived from resistant plants failed to interact with VPg (6, 11-13), suggesting that eIF4E and its interaction with VPg are important for potyvirus infection. In fact, *Arabidopsis* knockout mutants of eIF4E and its isoform, eIF(iso)4E, are resistant against potyviruses (14-16). Potyvirus mutants that overcame eIF4E-mediated resistance were reported to contain amino acid changes in VPg that restored its ability to bind to the

eIF4E produced by the resistant plants (5, 6, 13, 17). Besides VPg, other potyvirus proteins, the cylindrical inclusion (CI) protein (18, 19), the helper-component proteases (HC-Pro) (20) and P1 (21), have also been reported to be involved in eIF4E-mediated recessive resistance. There is disagreement as to how eIF4E and these potyviral factors interact with one other in potyvirus infection, and how these interaction networks are affected in resistant plants containing the recessive allele of eIF4E (22), so these topics require further examination. Tracking of GFP-tagged potyviruses revealed that avirulent potyviruses were defective in cell-to-cell movement at an early stage of virus infection, but it is not yet clear whether the defect was caused by direct inhibition of cell-to-cell movement or by inhibition of viral replication in the resistant plants (5, 21, 23-25).

There are other recessive resistance genes in pea that have not yet been cloned but do not seem to encode eIFs. The recessive resistance genes *cyv1* (resistance to ClYVV), *mo* (resistance to BYMV), and *sbm-2* (resistance to PSbMV) were mapped close to one another in pea linkage group (LG) II (26, 27). The *eIF(iso)4E* gene is also found in LG II (28). However, the recessive genes (i.e., *cyv1*, *mo*, and *sbm-2*) are not likely to be *eIF(iso)4E* because there was no difference in the deduced amino acid sequence of the eIF(iso)4E proteins between susceptible and resistant peas (26, 28). Thus, if virus isolates emerge that overcome these recessive resistance genes, the viral determinant responsible might not be VPg. In fact, the resistance conferred by *sbm-2* was overcome by PSbMV mutants that have mutations corresponding to the N-terminal part of the P3 protein (29, 30). In this study, breaking of the *cyv1* resistance by ClYVV was attributed to the P3 cistron.

Until recently, the functions of P3 have been poorly understood. Functional P3

82 protein was found to be recruited to the potyvirus replication complex (31) and to be
83 involved in accumulation of the virus (32, 33), symptomatology (34, 35), viral
84 microtubule-related inter- and intracellular movement (36), and determination of host range
85 (33). Few examples of interaction of P3 with host factors have been reported. However,
86 RuBisCO directly bound to P3, which led to decreases in plant chlorophyll contents and
87 photosynthesis (37, 38).

88 A small open reading frame (ORF) called PIPO (for Pretty Interesting *Potyviridae*
89 ORF) was found to be embedded in the P3 cistron; this ORF can form a functional protein,
90 P3N-PIPO, comprising the N-terminal amino acids of P3 followed by the amino acids
91 encoded by PIPO, which are added presumably through a +2 (or -1) ribosomal frameshift
92 or transcriptional slippage (39, 40). Thus, P3N-PIPO has the same N-terminal part (P3N) as
93 P3 and P3N-PIPO of *Turnip mosaic virus* (TuMV) appears to interact with CI in the
94 plasmodesmata of *Nicotiana benthamiana* and facilitate movement of viral RNA to
95 neighboring cells (40-42). These studies indicate that both P3 and P3N-PIPO are essential
96 proteins for potyvirus infection and thus have the potential to be the virulence determinant
97 in viruses that can overcome resistance in *cyv1* and *sbm-2* peas.

98 Previous studies have not revealed whether breaking of the *sbm-2* resistance
99 involves P3, P3N-PIPO, or both (29). Here, we genetically examined whether either P3 or
100 P3N-PIPO was involved in breaking of the *cyv1* resistance by ClYVV. We then
101 investigated the contribution of the P3 and P3N-PIPO proteins to breaking of the resistance
102 by producing these proteins in *trans*, using either an expression cassette containing the 35S
103 promoter or the *White clover mosaic virus* (WClMV) vector (43), and introducing these

into plants along with a ClYVV isolate that is normally avirulent to *cyv1* pea.

Materials and Methods

Construction of chimeric viruses and P3 transient expression cassettes

The infectious ClYVV clone pClYVV/C3-S65T-Sal (hereafter, Cl-no30) was made and modified from ClYVV isolate no. 30 in previous studies and contains a coding sequence for the green fluorescent protein (GFP) (44, 45). Since the original sequence of ClYVV isolate no. 30 (DDBJ/GenBank/EMBL accession number AB011819) contains two *Sal*I sites in the VPg and NIb cistrons and the site in VPg was utilized for constructing the chimeric viruses, the site in NIb was eliminated by site-directed mutagenesis prior to construction of the chimeric viruses. Seven chimeric viruses (Cl-P1HC, Cl-BB, Cl-NS, Cl-SB, RB, RB/P3^{KII}PIPO^{Q62}, and Cl/P3^{RAM}) were generated by replacing regions of Cl-no30 with the corresponding regions of 90-1 Br2 The cDNA sequences of 90-1 Br2 were amplified by RT-PCR using KOD-Plus 2 DNA polymerase (Toyobo, Osaka, Japan) with the following primers: UTR3′-s (GGATTGATGTGATATCTCCACTGACGTAAG); HCpro3′-as (GTTGCAAGTTCTCTCGTACC); HCbgl5′-s (ACGTGTACATCAGATCTCAATGTAAT); P3bgl3′-as (TTTTGATGTGAGATCTCACTTGACTC); P3nhe3′-s (TTCTTAATGTGCTAGCAACAATTACG); VPsal5′-as (TAGTCGCGCAAACCACTTATGCGATTTAGA); VPsal5′-s

126 (ACCATACAAGCTGAGGGACTCAAATGTTGT); and Polbam3′-as
127 (AGCTTGGGATCCTTTTTTTTTTCTCGCTCTATAAAGATCA). Recombinant plasmids
128 Cl-P1HC, Cl-BB, Cl-NS, and Cl-SB (Fig. 1) were created by insertion of 90-1 Br2 cDNA
129 sequences into the following restriction sites: for Cl-P1HC, the *Eco*RV site at the 5′-UTR
130 and the *Bgl*II site at the beginning of HC-Pro; for Cl-BB, the *Bgl*II sites within the HC-Pro
131 and P3 coding regions; for Cl-NS, the *Nhe*I site in the center of P3 and the *Sal*I site in the
132 center of VPg; and for Cl-SB, the *Sal* I site in VPg and the *Bam*HI site downstream of poly
133 A sequence.
134 The chimeric viruses RB, RB/P3^{KII}PIPO^{Q62}, and Cl/P3^{RAM}, which contain the P3
135 cDNA fragment of 90-1 Br2, were generated by the following steps. To generate RB, the
136 chimeric cDNA fragment composed of HC-Pro of Cl-no30 and P3 of 90-1 Br2 within the
137 *Bgl*II sites on HC-Pro and P3 was made by two-step PCRs with primers no30bgl-s
138 (CAGATCTCAATGTAGTCCAATGTGGTTCTG), no30br2-as
139 (CCAACTCTGTAAAACTTCAAATCTGACTC), no30br2-s
140 (GAGTCAGATTTGAAGTTTTACAGAGTTGG), and br2bgl-as
141 (CAGATCTCACTTGACTCAGAATGC). For the first step, primer pairs
142 no30bgl-s/no30br2-as and no30br2-s/br2bgl-as were used to amplify the cistrons encoding
143 HC-Pro and P3, respectively. Then, cDNAs of HC-Pro and P3 were fused with PCR by
144 using primer pair no30bgl-s/br2bgl-as. The fragment was cloned into a pGEM-T-Easy
145 vector (Promega, Madison, WI, USA) for making the chimeric virus RB.
146 To make RB/P3^{KII}PIPO^{Q62} and Cl/P3^{RAM}, the HC-Pro–P3 fragments were amplified by
147 two-step PCR as described above with the primers, except for br2P3_644-s

148 (GTAACAAGCATCAAGAATCAAGCAATC) and br2P3_644-as
149 (GATTGCTTGATTCTTGATGCTTGTTAC) for RB/P3^{KII}PIPO^{Q62} , and br2RAM-s
150 (GCAACAAGCATTAAAAACCAAGCAATC) and br2RAM-as
151 (GATTGCTTGGTTTTTAATGCTTGTTGC) for Cl/P3^{RAM}, instead of no30br2-s and
152 no30br2-as. These cloned fragments were inserted into vector Cl-no30 after digesting with
153 *Bgl*II.
154 To express in *trans* the genes for the proteins encoded by the P3 cistrons of
155 Cl-no30 and RB, we used two different systems: the plant transient expression vector
156 pE2113, which contains a 35S promoter for transgene expression (46), and the WClMV
157 vector (43). The restricted enzyme sites of *Bam*HI–*Sac*I and *Spe*I–*Xho*I were added to the 5′
158 and 3′ terminals of cDNA fragments of the P3 cistrons to insert them into the pE2113 and
159 WClMV vectors, respectively (43, 46). To construct P3 cistrons that exclusively produce
160 the P3N-PIPO protein (designated no30_P3N-PIPO and RB_P3N-PIPO), an adenosine
161 nucleotide was inserted at position 464, in the G_2A_6 , around which a frameshifting is
162 considered to occur, (GGAAAAAA → GGAAAAAAA) (39). To construct P3 cistrons that
163 exclusively produce the P3 protein (designated no30_P3ΔPIPO and RB_P3ΔPIPO), one
164 nucleotide was changed at position 477 to generate a stop codon in the PIPO reading frame
165 (AGA → TGA) without causing an amino acid change in the P3 ORF.
166 To additionally express P3 or P3N-PIPO from Cl-no30 in *cis*, no30_P3ΔPIPO and
167 no30_P3N-PIPO were inserted into the *Pst*I site of the infectious clone,
168 pClYVV-SeIF4E-GFP (3), instead of SeIF4E as follows. The *Pst*I site followed by the P1
169 C-terminal fragment and PstI-NIa-Pro digestion site were attached to the 5′- and 3′-termini

of the no30-P3ΔPIPO cDNA sequence by two-step PCR as described above using the primers no30_P1-Pst_s (5′-GCGCGCCTGCAGAAAAACTGAAAGTG-3′), Cl-no30P1P3_as (5′-GTCAATGATTTGCCAGAGAATTCT-3′), Cl-no30P1P3_s (5′-AGAATTCTCTGGCAAATCATTGAC-3′), and Cl-no30P3Cter-NIa_as (5′-GCGCCTGCAGATTGGAAAACAAATTTCATTTCCATGACAAACCACTTTGGTTC-3′). The amplified fragments were inserted into the vector pClYVV-SeIF4E-GFP after digestion with *Pst*I. The resulting construct was designated Cl/P3ΔPIPO (Fig. 5B).

Cl/P3N-PIPO was also generated using the primers no30_P1-Pst_s, Cl-no30P1P3_as, Cl-no30P1P3_s, and Cl-no30P3NPIPO-NIa_as (5′-GCGCCTGCAGATTGGAAAACAAATTTCATATGCTTGTTACTGAC-3′).

Virus inoculation and detection

We examined the ability of the constructed ClYVV chimeras to systemically infect *cyv1* pea plants as follows. The ClYVV cultures were recovered in broad beans (*Vicia faba*), which were biolistically inoculated with the constructed ClYVV infectious plasmids as described by Andrade et al (47). Infected upper leaves of broad bean were stored in a deep freezer and used as inoculum for inoculation of *cyv1* pea plants as described (47). Second to fourth upper leaves from bottom of *cyv1* pea plants two weeks old were mechanically inoculated. The movement of each virus was monitored with GFP fluorescence, which was observed for 5 days post inoculation (dpi) using an epifluorescence microscope (VB 7010; Keyence, Osaka, Japan). The presence of chimeric viruses in upper leaves was also

192 detected by reverse transcription (RT)-PCR, as described in (26). For RT-nested PCR, the
193 first PCR was performed with primers designed based on *NIb* of ClYVV,
194 5′-CTTTAGACCTATGATGGGC-3′ (sense) and 5′-GTTCAAGCCCAATTCTTTG-3′
195 (antisense); for the second PCR, the sense primer of first PCR and
196 5′-GTATATATGATCTCCGTGTAC-3′ (antisense) were used to detect ClYVV with
197 greater sensitivity.

198 We tested the infectivity of the constructed ClYVV chimeras and of Cl-no30 with
199 additional production in *trans* of proteins derived from P3 cistrons, as follows. Biolistic
200 inoculation of detached leaves of a *cyv1* pea line (PI 429853) with the ClYVV chimeric
201 clones, or co-inoculation of the Cl-no30 infectious clone with the pE2113 vectors, was
202 performed essentially as described by Andrade et al (47). Tungsten particles were coated
203 either with 1 μg of a ClYVV chimeric plasmid clone or with a mixture of 997 ng Cl-no30
204 and 3 ng of cloned pE2113 vector containing a P3 cistron (P3, P3N-PIPO, or P3ΔPIPO)
205 and bombarded into leaves of cultivar PI 429853. The virus infection was monitored by
206 GFP fluorescence from Cl-no30. The GFP fluorescence was observed for 5 dpi, as
207 described above.

208 We investigated the systemic infection of Cl-no30 co-inoculated with WClMV
209 vectors designed to exclusively produce the P3N-PIPO protein in the leaves of *cyv1* peas.
210 Biolistic co-inoculation of *cyv1* peas was performed with plasmid mixtures containing 800
211 ng of Cl-no30 and 200 ng of the WClMV expression vector carrying either
212 no30_P3N-PIPO or RB_P3N-PIPO. Infection by Cl-no30 was monitored by using GFP
213 fluorescence and by RT-PCR and RT-nested PCR for ClYVV NIb, as described above. To

monitor infection by WClMV, RT-PCR using primers specific for the coat protein (CP) of WClMV (i.e., CP-Nort-head and CP-Nort-tail) was performed as described by Ido (43). RT-PCR using primers specific for the multi-cloning site of WClMV, f (43), and Cl-P3-574as (5′-CTCTGGGCTAGTATTTTGGAATAC-3′ [antisense]) confirmed the stability of P3N-PIPO expression from the WClMV vector.

Antibody production and western blotting

To detect the P3N-PIPO protein by immunoblotting, antibodies were raised against the PIPO amino acid sequence fused with the maltose binding protein (MBP), which was produced by using the expression vector pMAL-c2 (New England Biolabs, Beverley, MA, USA). To generate this protein, the last 186 nucleotides of the P3N-PIPO ORF from Cl-no30, including the stop codon, were inserted downstream from the *malE* gene (which encodes MBP) of pMAL-c2, and the vector was transformed into *Escherichia coli* JM109. The transformants were cultured for 14 h in LB broth including 50 μg/mL ampicillin. The production of the gene's fusion protein was induced with 0.1 mM IPTG in fresh LB broth at 35°C for 4 h. Cell lysates were added to a ten-fold volume of 2× Laemmli buffer, heated for 3 min at 100°C, subjected to SDS-PAGE electrophoresis on a 10% Tris gel for 40 min, and stained with Coomassie Brilliant Blue. The MBP-fused PIPO protein (around 50 kDa) was used as the PIPO antigen. To confirm that the newly generated antibody was able to detect PIPO, a PIPO cDNA sequence lacking the G_2A_6 motif, which might cause a frameshifting, was inserted downstream of the region encoding glutathione S-transferase (GST) in expression vector pGEX (GE Healthcare, Piscataway, NJ). The GST-fused PIPO

was produced and subjected to SDS-PAGE as described above. The band, which migrated at around 33 kDa, was specifically detected by immunoblotting with the antibody as described previously (48), indicating that this antibody is able to detect PIPO (Fig. S1). We later found that the P3N-PIPO antibody could simultaneously detect both P3 and P3N-PIPO. We speculate that a ribosomal frameshift might have occurred in the G_2A_6 motif at the beginning of the PIPO sequence, resulting in the production of an MBP-fused P3 peptide along with the MBP-fused PIPO protein. The motif A_6G_1 has been reported to stimulate a –1 frameshift in *E. coli* (49).

To sensitively detect the P3N-PIPO protein derived from the infecting ClYVV in peas, a urea-containing buffer was used to prepare the samples for immunoblotting, as described previously (50). Uninoculated upper leaves with symptoms were harvested at 9 dpi, ground in liquid nitrogen, and denatured in 12-fold (w/v) urea denaturing buffer containing 4.5 M urea, 1% (v/v) Triton X-100, 0.5% DTT, 0.00625 M Tris-HCl pH 6.8, 2% (w/v) SDS, 5% mercaptoethanol, 5% sucrose, and 0.002% bromophenol blue. The plant lysates were analyzed by SDS-PAGE, as described by Atsumi et al (48).

In vitro transcription

In the plasmids pE2113/no30_P3 and pE2113/RB_P3, the 5′ end of the P3 sequence harbored a *Bam*HI restriction site and the start codon (5′-GGATCCACCATG + P3 sequence), while its 3′ end harbored the stop codon (TAA) and a *Sac*I site (P3 sequence + TAAGAGCTC-3′). The P3 regions of Cl-no30 and RB were cloned into the pSP64 Poly(A)

vector (Promega) using *Bam*HI and *Sac*I. The resulting plasmids, pSP-WT-P3 and pSP-RB-P3, were used as templates for *in vitro* transcription. The plasmid DNAs were linearized with *Eco*RI and extracted with phenol/chloroform (1:1 v/v) followed by ethanol precipitation. RNA was synthesized from the linearized DNA using an AmpliCap SP6 High Yield Message Maker Kit (Cellscript Inc., Madison, WI, USA) in the presence of a cap analog, according to the manufacturer's instructions.

In vitro translation

As an *in vitro* translation system, MM2dL, an extract derived from *Arabidopsis* MM2d cells (51), was utilized. To obtain MM2dL, the protocol to prepare a tobacco BY-2 cell-derived extract (52, 53) was applied. The translation reaction cocktails (15 μl) for MM2dL included 7.5 μl of MM2dL, 1 μl of 15× Substrate Mix (11.25 mM ATP, 1.5 mM GTP, 375 mM creatine phosphate, 375 μM each of 19 amino acids excluding methionine, and 1.2 mM spermine), 3 μg of creatine phosphokinase (Roche Diagnostics, Indianapolis, IN, USA), 12 U of RNasin, ~500 ng of mRNA, and 0.3 μl of [^{35}S]methionine (43.5 TBq mmol^{-1}; American Radiolabeled Chemicals, St. Louis, MO, USA). The volume was adjusted with TR buffer [30 mM HEPES-KOH (pH 7.4), 80 mM potassium acetate, 1.8 mM magnesium acetate, 2 mM dithiothreitol, and one tablet of Complete Mini protease inhibitor (Roche Diagnostics) per 10 ml of mixture] (52, 53). The mixtures were incubated at 25°C for 120 min.

After incubation, the translation products were separated on a NuPAGE 4–12%

Bis-Tris Gel (Invitrogen, Carlsbad, CA, USA) with MES running buffer (Invitrogen). The protein bands were visualized using a FLA-7000 image analyzer (Fuji Photo Film, Tokyo, Japan). The acquired images were processed using MultiGauge (Fuji Photo Film) and Photoshop 12.0.4 (Adobe Systems Inc., San Jose, CA, USA).

Results

The breaking of the *cyv1* resistance by ClYVV isolate 90-1 Br2 was attributed to the region encoding the P3 and P3N-PIPO proteins

Pisum sativum cultivar PI 429853, which carries recessive resistance gene *cyv1*, is resistant to Cl-no30 (26). The resistance of *cyv1* can be broken by isolate 90-1 Br2: *cyv1* pea infected with 90-1 Br2 showed chlorotic spots on the upper leaves at 5 weeks post inoculation (wpi). 90-1 Br2 induced more severe symptoms, including dwarfing and necrosis, in susceptible pea cultivar PI 250438 (47) than did Cl-no30 (Fig. 1B). To address which gene is responsible for breaking of the *cyv1* resistance, we compared the entire nucleotide sequence of the polyprotein-coding region between Cl-no30 (AB011819) and 90-1 Br2 (AB732962) and found 483 nucleotide differences dispersed throughout the genomes.

We then created four chimeric viruses in which sequences from the Cl-no30 infectious clone were replaced with the corresponding sequences from 90-1 Br2 (44); these chimeras contained the 90-1 Br2 sequence from the 5′-UTR to HC-Pro (Cl-P1HC), from

302 HC-Pro to P3 (Cl-BB), from P3 to 6K2 (Cl-NS), and from 6K2 to 3′-poly A (Cl-SB) (Fig.
303 1). These four viruses were inoculated into the *cyv1* pea cultivar PI 429853 and observed
304 for 6 wpi. After 5 wpi, the peas inoculated with Cl-BB showed chlorotic spots and GFP
305 fluorescence in the upper leaves (Fig. 1) but the other chimeric viruses could not overcome
306 *cyv1* resistance (Fig. 1). The virulence of Cl-BB against *cyv1* appeared to be comparable to
307 that of 90-1 Br2 (Fig. 1). Cl-BB contained most of the HC-Pro cistron sequence of 90-1
308 Br2, but this sequence was also present in Cl-P1HC, which could not overcome
309 *cyv1*-mediated resistance, so we hypothesized that breaking of the resistance by Cl-BB was
310 caused by the chimeric sequence of the P3 cistron, which was unique to Cl-BB. To test this
311 hypothesis, we created one more chimeric ClYVV called Resistance Breaking (RB) which
312 contained the same part of the P3 cistron from 90-1 Br2 as was present in Cl-BB, and we
313 confirmed that RB broke *cyv1* resistance (Figs. 1 and 2) as did 90-1 Br2 and Cl-BB. Thus,
314 we concluded that the P3 cistron of 90-1 Br2 was responsible for its ability to break the
315 resistance conferred by *cyv1*.
316
317 **Both P3 and P3N-PIPO were involved in breaking of the *cyv1* resistance**
318
319 The P3 cistron has been reported to produce two proteins, P3 and P3N-PIPO,
320 which have the same N-terminal sequence (39, 40). Thus, we designed experiments to test
321 which protein is responsible for breaking of the resistance. There were 58 nucleotide
322 differences between the mapped P3 regions of Cl-no30 and RB (Fig. 3). A total of 47 were
323 synonymous with respect to both proteins, and nine caused seven differences in amino acid

residues in P3 but not in PIPO (Fig. 3A, yellow boxes, and 3B; hereafter, "PIPO" refers to the amino acid region unique to P3N-PIPO.) Two of the nucleotide differences in P3 were synonymous with the P3 protein, but caused two differences in the amino acid sequences of PIPO (Fig. 3A, orange boxes, and 3C). None of the nucleotide differences caused a change in amino acid residue simultaneously in P3 and PIPO. Thus, the nucleotide sequence comparisons did not indicate whether P3N-PIPO, P3, or both are involved in the breaking of *cyv1*-mediated resistance.

We further investigated the possible role of P3N-PIPO in breaking of the resistance. To do this, we used two nucleotide sequence differences that caused an amino acid change in PIPO between Cl-no30 and RB, but did not affect the amino acid sequence of P3. We made PIPO point mutants of Cl-no30 and RB by introducing either or both of the nucleotide substitutions into the genomic cDNA of the infectious clones. The point mutants were independently inoculated into *cyv1* pea plants, and the ability of the clones to infect upper (uninoculated) leaves was tested by means of GFP fluorescence observation, RT-PCR, and RT-nested PCR. These mutations, corresponding to amino acids 38 and 62 of PIPO, altered the virulence of both Cl-no30 and RB in the *cyv1* pea plants. A substitution at position 38 in the PIPO amino acid sequence of RB (ATT [isoleucine] → A<u>C</u>T [threonine]; RB/PIPO^{I38T}) dramatically reduced its virulence in *cyv1* peas but the opposite substitution (threonine to isoleucine) in Cl-no30 (Cl/PIPO^{T38I}) had no effect (Fig. 4A). Conversely, a substitution at position 62 (TAA [stop codon] → <u>C</u>AA [glutamine]; Cl/PIPO^{62Q}) partially conferred virulence on Cl-no30 but the opposite substitution (glutamine to a stop codon; RB/PIPO^{Q62}) had no detrimental effect on RB. The mutants in which both substitutions

346 were simultaneously induced (Cl/PIPO$^{T38I, 62Q}$ and RB/PIPO$^{I38T, Q62}$), had similar virulence
347 to the single-point mutants Cl/PIPO^{62Q} and RB/PIPO^{I38T}, respectively (Fig. 4A). These
348 results genetically demonstrated the involvement of P3N-PIPO in the breaking of resistance
349 in *cyv1* pea. In addition to 90-1 Br2, we found three other ClYVV isolates (I89-1
350 [AB732963], N [AB732964], and MB3 [AB732965]) that could break *cyv1* resistance.
351 Among these four isolates, both isoleucine-38 and glutamine-62 were conserved (Fig. 3C),
352 supporting the importance of these positions for breaking of the *cyv1* resistance. However,
353 with respect to the infection of *cyv1* pea plants, none of the point mutants of Cl-no30 tested
354 here gained virulence that was comparable to that of RB, and none of the point mutants of
355 RB completely lost systemic infectivity to the degree seen in Cl-no30, suggesting the
356 involvement of other parts of the P3N-PIPO protein or of P3 in breaking of the resistance.
357 We thus investigated the possible role of the P3 protein in breaking of the
358 resistance. An RB mutant in which nucleic acid substitutions changed 4 amino acid
359 residues in the P3 protein and eliminated the final 15 amino acid residues in the PIPO
360 protein by adding a stop codon (Fig. 4B, RB/P3^{KII}PIPO^{Q62}), reduced virulence in *cyv1* peas.
361 Since elimination of the final 15 amino acid residues alone (Fig. 4A, RB/PIPO^{Q62}) did not
362 affect the virulence of RB, the reduced virulence of RB/P3^{KII}PIPO^{Q62} was assumed to be
363 caused by the four amino acid substitutions in the P3 protein. A Cl-no30 mutant containing
364 three amino acid substitutions that only affected the P3 protein (Fig. 4B, Cl/P3^{RAM}), making
365 it more like that of RB, was able to partially break *cyv1* resistance (Fig. 4B). The results
366 indicated that the P3 protein is also involved in breaking of the resistance conferred by
367 *cyv1*.

368 We obtained additional genetic evidence indicating that both P3 and P3N-PIPO
369 were important for breaking of the resistance. Peas carrying *cyv1* showed resistance to
370 ClYVV isolate 90-1, but it could sometimes overcome *cyv1* resistance. Isolate 90-1 Br2
371 emerged from systemic leaves of such a *cyv1* pea infected with 90-1. Comparing the
372 genomic sequence of the P3 cistron of 90-1 with that of 90-1 Br2, we found only one point
373 mutation, which caused a substitution (arginine to methionine) at position 28
374 (P3&P3N-PIPO^{R28M}) of the P3 and P3N-PIPO proteins of 90-1, implying that this point
375 mutation enabled 90-1 Br2 to overcome *cyv1*. As expected, a point mutant of RB in which
376 the methionine at position 28 was substituted with arginine (RB/P3&P3N-PIPO^{M28R}) failed
377 to overcome *cyv1* resistance (Fig. 4C). However, the difference between RB and Cl-no30 in
378 virulence to cyv1 pea could not be attributed exclusively to the point mutation at position
379 28. The amino acid residue at position 28 of P3 in Cl-no30 was found to be lysine, so we
380 introduced mutations into Cl-no30 and RB that changed the lysine of P3 and P3N-PIPO of
381 Cl-no30 to methionine (Cl/P3&P3N-PIPO^{K28M}) and the methionine of these proteins in RB
382 to lysine (RB/P3&P3N-PIPO^{M28K}), and inoculated these viruses into *cyv1* peas (Fig. 4C).
383 These substitutions did not affect virulence in *cyv1* peas: Cl/P3&P3N-PIPO^{K28M} still failed
384 to overcome *cyv1*-mediated resistance and RB/P3&P3N-PIPO^{M28K} still infected the *cyv1*
385 peas systemically (Fig. 4C).
386
387 **Importance of P3N-PIPO for ClYVV cell-to-cell movement in *cyv1* peas**
388
389 We have previously shown that cyv1 restricts Cl-no30 to single cells (26). Because

RB breaks *cyv1* resistance and results in systemic infection, it should no longer be restricted to the initially infected cells. To confirm this assumption, GFP-tagged Cl-no30 and RB were biolistically inoculated into *cyv1* peas. The GFP fluorescence of RB around the initially infected cells was able to spread to neighboring cells, but almost no movement was detected for Cl-no30 (Table 1). Next, we biolistically inoculated *cyv1* peas with the P3N-PIPO point mutants of Cl-no30 and RB. The substitution of isoleucine with threonine at position 38 of PIPO in RB (RB/PIPO^{I38T}, Fig. 4A) impaired its cell-to-cell movement (Table 1), whereas the opposite substitution in Cl-no30 (Cl/PIPO^{T38I}, Fig. 4A) had no effect on its cell-to-cell movement (Table 1). Conversely, although the substitution at position 62 in RB (RB/PIPO^{Q62}, Fig. 4A) had little effect on its cell-to-cell movement (Table 1), the opposite substitution in Cl-no 30 (Cl/PIPO^{62Q}, Fig. 4A) increased its efficiency of cell-to-cell movement almost to that of RB (Table 1). These results demonstrated that in *cyv1* pea, the cell-to-cell movement rate of the P3N-PIPO point mutants is correlated with the rate of systemic infection, suggesting that if a ClYVV isolate is able to move to adjacent cells in a *cyv1* pea, the virus infects systemically.

Quantitative involvement of P3N-PIPO in cell-to-cell and systemic movement of ClYVV in *cyv1* pea

The genetic analyses described above suggested the involvement of both P3 and P3N-PIPO proteins in breaking of the *cyv1* resistance. However, this interpretation did rule out the possibility that the differences between the genomic sequences of RB and Cl-no30,

412 rather than the amino acid sequences of the encoded proteins, were responsible for breaking
413 of the resistance. To confirm the involvement of the P3 and P3N-PIPO proteins, the
414 GFP-tagged Cl-no30 infectious clone was biolistically inoculated into *cyv1* peas together
415 with one of six transient expression cassettes. These cassettes were expected to produce the
416 P3 protein accompanied by a small amount of P3N-PIPO protein produced from the
417 occasional frameshift (pE2113/P3), the P3N-PIPO protein and a small amount of the P3
418 protein (pE2113/P3N-PIPO), or the P3 protein only (pE2113/P3ΔPIPO). A cassette of each
419 type was derived from both Cl-no30 and RB. The movement of Cl-no30 was monitored by
420 following the GFP fluorescence. Interestingly, the frequency of cell-to-cell movement of
421 Cl-no30 markedly increased when the P3N-PIPO protein from either Cl-no30 or RB was
422 expressed in *trans* (Fig. 5A and Table 2). The P3 protein from RB also seemed to enhance
423 the cell-to-cell movement of Cl-no30, although to a lesser extent (Fig. 5A and Table 2). In
424 particular, the fact that the increased expression of P3N-PIPO, even that from Cl-no30,
425 facilitated the cell-to-cell movement of Cl-no30 suggested a quantitative involvement of the
426 P3N-PIPO protein in breaking of the resistance. To confirm the quantitative involvement of
427 P3N-PIPO, we additionally inserted either of the modified Cl-no30 P3 cistrons, which
428 exclusively produced P3N-PIPO (Cl/P3N-PIPO) or P3 (Cl/P3ΔPIPO), into the GFP-tagged
429 Cl-no30 infectious clone (Fig. 5B). Cl/P3N-PIPO and Cl/P3ΔPIPO were genetically
430 expected to produce more P3N-PIPO and P3, respectively, than the parental clone
431 (Cl-no30) in infected plants. These constructs were biolistically inoculated into *cyv1* pea
432 plants and their GFP fluorescence was observed for 3 dpi. As expected, Cl/P3N-PIPO
433 moved more frequently to neighboring cells than did Cl/P3ΔPIPO and Cl-no30 (Fig. 5B

434 and Table 1). This result led us to hypothesize that RB can break *cyv1* resistance, resulting
435 in systemic infection, by producing more P3N-PIPO protein than Cl-no30.
436 We examined this hypothesis in the following experiments. First, we compared the
437 levels of P3N-PIPO at 9 dpi in susceptible pea (PI 250438) infected with Cl-no30 or RB.
438 As shown in Fig. 6A, P3 and P3N-PIPO were detected at about 40 and 24 kDa, respectively.
439 Compared with P3, which accumulated to comparable levels in both isolates, P3N-PIPO
440 was detected only in the RB-infected peas but not in the Cl-no30 infected peas (Fig. 6A).
441 There were a few faint bands, one of which might have been P3N-PIPO, between 20 and 25
442 kDa in the sample from Cl-no30 (Fig. 6A, Experiment 1), but none of them had a
443 comparable intensity to that of RB P3N-PIPO. We then compared the accumulation levels
444 of P3N-PIPO produced from the P3 cistrons between Cl-no30 and RB using an *in vitro*
445 translation system and obtained results that were consistent with those of our *in vivo*
446 analysis. P3N-PIPO from RB P3 was detected at about 24 kDa, but that from Cl-no30 P3
447 (at about 21 kDa) was not detected (Fig. 6C, lanes P3 of Cl-no30 and RB), suggesting a
448 difference in efficiency of P3N-PIPO production between Cl-no30 and RB. Although both
449 experiments failed to detect P3N-PIPO from Cl-no30, we believe that Cl-no30 produced
450 P3N-PIPO in the infected peas but that its accumulation was not detectable because
451 P3N-PIPO has been reported to be essential for the cell-to-cell movement of potyviruses
452 (42, 54), and a point mutant of Cl-no30 that no longer produced P3N-PIPO failed to
453 systemically infect peas inoculated with it (unpublished data). We therefore conclude that
454 P3N-PIPO accumulated to a higher level in the RB-infected pea plants than in the
455 Cl-no30-infected pea plants.

We then examined whether the presence of additional P3N-PIPO protein would enable Cl-no30 to infect *cyv1* peas systemically by using WClMV vectors. The *cyv1* peas were co-inoculated with Cl-no30 and a WClMV vector designed to produce the P3N-PIPO protein of either Cl-no30 (WCl/no30_P3N-PIPO) or RB (WCl/RB_P3N-PIPO); thus, the additional P3N-PIPO protein was systemically independent of Cl-no30 in the inoculated *cyv1* peas. Although we failed to detect any GFP signals in the upper leaves of the inoculated *cyv1* peas, RT-PCR and RT-nested PCR detected Cl-no30 in the upper leaves of the *cyv1* peas inoculated with WClMV that produced the P3N-PIPO protein of either Cl-no30 or RB at 11 dpi (Fig. 7). Cl-no30 was not able to infect *cyv1* peas systemically when the *cyv1* peas were co-inoculated with the WClMV empty vector (Fig. 7). Here, we should note that co-inoculation of Cl-no30 and WCl/no30_P3N-PIPO or WCl/RB_P3N-PIPO did not always result in systemic infection of *cyv1* peas with both viruses. This failure of systemic infection might be explained by an effect-related to RNA-mediated cross protection (55) because Cl-no30 is unrelated with WClMV but shares the nucleotide sequence of P3 with WCl/no30_P3N-PIPO and WCl/RB_P3N-PIPO. Even so Cl-no30 could spread systemically in *cyv1* peas when WCl/no30_P3N-PIPO and WCl/RB_P3N-PIPO spread systemically (Fig. 7). These results are consistent with the enhanced cell trafficking of Cl-no30 caused by additional P3N-PIPO protein from either Cl-no30 or RB produced in a pE2113 transient expression vector and Cl/P3N-PIPO (Fig. 5, Table 1 and 2).

Discussion

In this study, we genetically mapped the region involved in the breaking of *cyv1*-mediated resistance by using chimeric ClYVVs constructed from isolates that were virulent and avirulent to *cyv1* peas, and we revealed that the P3 cistron was the determinant for breaking of the resistance. Because the P3 cistron had recently been shown to encode two proteins, P3 and P3N-PIPO (39), we introduced point mutations that were synonymous with respect to the P3 protein but non-synonymous with respect to the P3N-PIPO protein, and vice versa, into RB and Cl-no30 infectious clones. Genetic analysis with these point mutants suggested that both P3 and P3N-PIPO were involved in breaking of the resistance (Fig. 4). Moreover, additional P3N-PIPO protein produced in *cis* and *trans* enabled the simultaneously inoculated Cl-no30 virus to move not only to neighboring cells but also systemically, to other leaves, in *cyv1* peas (Figs. 5 and 7 and Tables 1 and 2). Therefore, we clearly showed that the P3N-PIPO protein is a virulence determinant of ClYVV in *cyv1* peas. The P3 cistron has been shown to be a determinant of the host range of TuMV (33, 34) and of potyvirus virulence in plants with dominant and recessive resistance (29, 30, 56). However, they did not examine whether P3 or P3N-PIPO were responsible for the determination of host range and potyvirus virulence. This is the first report showing that the P3N-PIPO protein is a virulence determinant in plants resistant to potyviruses.

Among the known recessive potyvirus resistance genes in pea, *cyv1* and *sbm-2* have not yet been identified (26-28). On the other hand, the recessive resistance genes *cyv2* (against ClYVV); *sbm-1*, *-3*, and *-4* [against pea seed-borne mosaic virus (PSbMV)]; and *wlv* [against bean yellow mosaic virus (BYMV)] are identical or allelic to one another, and

all encode pea homologs of eIF4E in LG VI (3-5, 27). As in pathosystems between other potyviruses and eIF4E family-mediated recessive resistance in plants, in most cases VPg has been reported to be the virulence determinant of PSbMV and BYMV in these resistant peas, although ClYVV P1 was the determinant in *cyv2* peas (4, 5, 21). Regarding the possible relationship and functions of *cyv1*, *sbm-2*, and *mo*, Gao et al. (28) reported that a candidate gene, *eIF(iso)4E*, is located in the same linkage group as *sbm-2* and *mo*. However, because no differences have been detected in the deduced amino acid sequences of eIF(iso)4E between susceptible and resistant peas, *cyv1* and *sbm-2* do not likely encode eIF(iso)4E (26, 28). Consistent with this, the P3 cistron but not VPg of PSbMV P-2 was associated with the breaking of *sbm-2* resistance in the *P. sativum* cultivar Dark Skinned Perfection (29, 30), as we found for the virulence determinants of ClYVV in *cyv1* pea plants.

Then what protein does *cyv1* encode and how do P3 and P3N-PIPO interact with it to break *cyv1* resistance? A couple of mechanisms involving recessive resistance to viruses have been proposed. First, mutations may occur in a plant gene that encodes a repressor of anti-viral defense systems. Second, mutations may arise that disrupt the function of an allele-encoding protein that supports viral infection and spread in a plant. The latter case has been well documented for mutant alleles encoding eIFs in several crops showing recessive resistance against potyviruses (17). To our knowledge, there is no report regarding an association of P3 and P3N-PIPO with the repression of anti-viral defenses. We thus stand by the latter possibility (i.e., P3 and P3N-PIPO may interact with a *cyv1*-encoding protein that is a co-opted host factor for ClYVV infection in pea). Several

522 recent studies have revealed distinct aspects of P3 and P3N-PIPO functions and properties.
523 P3 is localized in the endoplasmic reticulum and Golgi and is colocalized into vesicles
524 induced by a 6-kDa potyvirus membrane protein (6K) that contain viral RNA and viral
525 replicase components (57). P3 traffics along actin filaments and plays a role in intra- and
526 intercellular movement (36). On the other hand, P3N-PIPO is localized in plasmodesmata
527 and recruits the CI protein to plasmodesmata, which probably facilitates cell-to-cell
528 movement (42). P3N-PIPO has been recently shown to be required for cell-to-cell
529 movement of potyviruses (42, 54), and the resistance mode of pea carrying *cyv1* and *sbm-2*
530 is to restrict avirulent ClYVV and PSbMV to the initially infected cells (26, 30). Taken
531 together, these studies raise the possibility that *cyv1* and *sbm-2* are allelic and encode a
532 co-opted host factor that is involved in replication, intra- and intercellular movement of
533 potyviruses and interacts with P3 or P3N-PIPO.
534 ClYVV isolate 90-1 Br2, which broke the resistance of *cyv1*, was more virulent
535 toward susceptible pea PI 250438 than Cl-no30 (Fig. 1B). We have recently mapped the
536 genomic region responsible for the higher virulence in susceptible pea using these chimeric
537 ClYVVs shown in Fig. 1A and found that the P3 cistron of 90-1 Br2 was responsible for its
538 higher virulence and RB accumulated more and spread more rapidly than did Cl-no30 (G.
539 Atsumi, unpublished data). These results support the possibility that P3 and P3N-PIPO
540 were involved in viral virulence through interaction with a co-opted host factor for ClYVV
541 infection. One such host factor is *Arabidopsis* PCaP1, which has been recently identified as
542 the plasma membrane protein that interacts with P3N-PIPO to facilitate cell-to-cell
543 movement of TuMV (40).

544 The quantitative involvement of the P3N-PIPO protein in breaking of the *cyv1*
545 resistance (Figs. 5, 6 and 7, and Tables 1 and 2) is unexpected characteristics, and
546 interesting findings were made in this study. We initially expected that concurrent
547 expression (in *trans*) of P3N-PIPO derived from the virulent ClYVV RB with avirulent
548 Cl-no30 might contribute to the virulence of Cl-no30 in *cyv1* peas, but that P3N-PIPO from
549 Cl-no30 would have little effect. However, the P3N-PIPO proteins derived from both RB
550 and Cl-no30 facilitated the cell-to-cell movement of Cl-no30 (Fig. 5). Moreover, additional
551 systemic production of P3N-PIPO, even that from avirulent Cl-no30, by using a WClMV
552 vector enabled simultaneously inoculated Cl-no30 to move systemically to upper leaves
553 (Fig. 7). These findings suggested that the more P3N-PIPO is produced by ClYVV, the
554 higher its virulence in *cyv1* peas. Indeed, RB produced higher levels of P3N-PIPO protein
555 than did Cl-no30 in susceptible pea (Fig. 6A and 6C), which might explain how RB was
556 able to break *cyv1*-mediated resistance.
557 How did high levels of P3N-PIPO contribute to breaking of the resistance?
558 P3N-PIPO recruits CI to plasmodesmata in a dose-dependent manner (42), and both CI and
559 P3N-PIPO are essential for cell-to-cell movement of potyvirus (54, 58). These studies offer
560 a possible explanation, namely that P3N-PIPO is defective in recruiting CI to
561 plasmodesmata, perhaps due to inefficient accumulation or localization of P3N-PIPO to the
562 plasmodesmata in *cyv1* peas, but that the higher levels of P3N-PIPO produced by RB
563 complement the defect and confer the ability for cell-to-cell movement on RB, thus
564 overcoming *cyv1*-mediated resistance.
565 The next question concerns how RB produces high levels of P3N-PIPO. We

showed that the level of P3N-PIPO produced by the P3 cistron derived from RB was higher than that derived from Cl-no30 through an *in vitro* translation assay (Fig. 6C). This result is in agreement with the increased accumulation of P3N-PIPO in RB-infected susceptible pea (Fig. 6A). Although our *in vitro* assay was insufficient to clarify whether P3N-PIPO is produced by a ribosomal frameshift or transcriptional slippage, several important features of P3N-PIPO expression were revealed: 1) the P3 cistron was sufficient and other regions of the viral genome were not required for the production of P3N-PIPO, and 2) the nucleotide differences in the P3 cistron between RB and no30 affected the efficiency of P3N-PIPO production. Together with our other results, we believe that RB acquired virulence to *cyv1* peas in part by producing an increased amount of P3N-PIPO. Using this experimental system, the mechanism of how P3N-PIPO is produced from the potyvirus genome will be elucidated in the near future.

Acknowledgements

This work was supported by the Japan Society for the Promotion of Science (JSPS) and the Ministry of Education, Culture, Sports, Science, and Technology of Japan (18108001, 20688002, 11J40125 and 22119006). Y. H.-K. was supported by JSPS. We used the Radioisotope Laboratory of Graduate School of Agriculture, Hokkaido University.

References

1. **Diaz-Pendon JA, Truniger V, Nieto C, Garcia-Mas J, Bendahmane A, Aranda MA.** 2004. Advances in understanding recessive resistance to plant viruses. Mol. Plant Pathol. **5:**223-233.

2. **Truniger V, Aranda MA.** 2009. Recessive resistance to plant viruses. Adv. Virus Res. **75:**119-159.

3. **Andrade M, Abe Y, Nakahara KS, Uyeda I.** 2009. The *cyv-2* resistance to *Clover yellow vein virus* in pea is controlled by the eukaryotic initiation factor 4E. J. Gen. Plant Pathol. **75:**241-249.

4. **Bruun-Rasmussen M, Møller IS, Tulinius G, Hansen JK, Lund OS, Johansen IE.** 2007. The same allele of translation initiation factor 4E mediates resistance against two *Potyvirus* spp. in *Pisum sativum*. Mol. Plant Microbe Interact. **20:**1075-1082.

5. **Gao Z, Johansen E, Eyers S, Thomas CL, Noel Ellis TH, Maule AJ.** 2004. The potyvirus recessive resistance gene, *sbm1*, identifies a novel role for translation initiation factor eIF4E in cell-to-cell trafficking. Plant J. **40:**376-385.

6. **Charron C, Nicolaï M, Gallois JL, Robaglia C, Moury B, Palloix A, Caranta C.** 2008. Natural variation and functional analyses provide evidence for co-evolution between plant eIF4E and potyviral VPg. Plant J. **54:**56-68.

7. **Léonard S, Viel C, Beauchemin C, Daigneault N, Fortin MG, Laliberté JF.** 2004. Interaction of VPg-Pro of *Turnip mosaic virus* with the translation initiation factor 4E and the poly(A)-binding protein *in planta*. J. Gen. Virol. **85:**1055-1063.

8. **Ruffel S, Caranta C, Palloix A, Lefebvre V, Caboche M, Bendahmane A.** 2004. Structural analysis of the eukaryotic initiation factor 4E gene controlling potyvirus resistance in pepper: exploitation of a BAC library. Gene **338:**209-216.

9. **Ruffel S, Gallois JL, Lesage ML, Caranta C.** 2005. The recessive potyvirus resistance gene *pot-1* is the tomato orthologue of the pepper *pvr2-eIF4E* gene. Mol. Genet. Genomics **274:**346-353.

10. **Kang BC, Yeam I, Jahn MM.** 2005. Genetics of plant virus resistance. Annu. Rev. Phytopathol. **43:**581-621.

11. **Léonard S, Plante D, Wittmann S, Daigneault N, Fortin MG, Laliberté JF.** 2000. Complex formation between potyvirus VPg and translation eukaryotic initiation factor 4E correlates with virus infectivity. J. Virol. **74:**7730-7737.

12. **Wittmann S, Chatel H, Fortin MG, Laliberté JF.** 1997. Interaction of the viral protein genome linked of turnip mosaic potyvirus with the translational eukaryotic initiation factor (iso) 4E of *Arabidopsis thaliana* using the yeast two-hybrid system. Virology **234:**84-92.

13. **Yeam I, Cavatorta JR, Ripoll DR, Kang BC, Jahn MM.** 2007. Functional dissection of naturally occurring amino acid substitutions in eIF4E that confers recessive potyvirus resistance in plants. Plant Cell **19:**2913-2928.

14. **Duprat A, Caranta C, Revers F, Menand B, Browning KS, Robaglia C.** 2002. The *Arabidopsis* eukaryotic initiation factor (iso)4E is dispensable for plant growth but required for susceptibility to potyviruses. Plant J. **32:**927-934.

15. **Lellis AD, Kasschau KD, Whitham SA, Carrington JC.** 2002.

632 Loss-of-susceptibility mutants of *Arabidopsis thaliana* reveal an essential role for
633 eIF(iso)4E during potyvirus infection. Curr. Biol. **12:**1046-1051.
634 16. **Sato M, Nakahara K, Yoshii M, Ishikawa M, Uyeda I.** 2005. Selective
635 involvement of members of the eukaryotic initiation factor 4E family in the
636 infection of *Arabidopsis thaliana* by potyviruses. FEBS Lett. **579:**1167-1171.
637 17. **Robaglia C, Caranta C.** 2006. Translation initiation factors: a weak link in plant
638 RNA virus infection. Trends Plant Sci. **11:**40-45.
639 18. **Abdul-Razzak A, Guiraud T, Peypelut M, Walter J, Houvenaghel M,**
640 **Candresse T, Le Gall O, German-Retana S.** 2009. Involvement of the cylindrical
641 inclusion (CI) protein in the overcoming of an eIF4E-mediated resistance against
642 *Lettuce mosaic potyvirus*. Mol. Plant Pathol. **10:**109-113.
643 19. **Tavert-Roudet G, Abdul-Razzak A, Doublet B, Walter J, Delaunay T,**
644 **German-Retana S, Michon T, Le Gall O, Candresse T.** 2012. The C terminus of
645 lettuce mosaic potyvirus cylindrical inclusion helicase interacts with the viral VPg
646 and with lettuce translation eukaryotic initiation factor 4E. J. Gen. Virol.
647 **93:**184-193.
648 20. **Roudet-Tavert G, Michon T, Walter J, Delaunay T, Redondo E, Le Gall O.**
649 2007. Central domain of a potyvirus VPg is involved in the interaction with the host
650 translation initiation factor eIF4E and the viral protein HcPro. J. Gen. Virol.
651 **88:**1029-1033.
652 21. **Nakahara KS, Shimada R, Choi SH, Yamamoto H, Shao J, Uyeda I.** 2010.
653 Involvement of the P1 cistron in overcoming eIF4E-mediated recessive resistance

against *Clover yellow vein virus* in pea. Mol. Plant Microbe Interact. **23:**1460-1469.

22. **Wang A, Krishnaswamy S.** 2012. Eukaryotic translation initiation factor 4E-mediated recessive resistance to plant viruses and its utility in crop improvement. Mol. Plant Pathol. **13:**795-803.

23. **Candresse T, Le Gall O, Maisonneuve B, German-Retana S, Redondo E.** 2002. The use of green fluorescent protein-tagged recombinant viruses to test *Lettuce mosaic virus* resistance in Lettuce. Phytopathology **92:**169-176.

24. **German-Retana S, Walter J, Le Gall O.** 2008. *Lettuce mosaic virus*: from pathogen diversity to host interactors. Mol. Plant Pathol. **9:**127-136.

25. **Nicaise V, German-Retana S, Sanjuán R, Dubrana MP, Mazier M, Maisonneuve B, Candresse T, Caranta C, LeGall O.** 2003. The eukaryotic translation initiation factor 4E controls lettuce susceptibility to the Potyvirus *Lettuce mosaic virus*. Plant Physiol. **132:**1272-1282.

26. **Choi SH, Nakahara KS, Andrade M, Uyeda I.** 2012. Characterization of the recessive resistance gene *cyv1* of *Pisum sativum* against *Clover yellow vein virus*. J. Gen. Plant Pathol. **78:**269-276.

27. **Provvidenti R, Hampton RO.** 1991. Chromosomal distribution of genes for resistance to seven potyviruses in *Pisum sativum*. Pisum Genetics **23:**26-28.

28. **Gao Z, Eyers S, Thomas C, Ellis N, Maule A.** 2004. Identification of markers tightly linked to *sbm* recessive genes for resistance to *Pea seed-borne mosaic virus*. Theor. Appl. Genet. **109:**488-494.

29. **Hjulsager CK, Olsen BS, Jensen DM, Cordea MI, Krath BN, Johansen IE,**

Lund OS. 2006. Multiple determinants in the coding region of *Pea seed-borne mosaic virus* P3 are involved in virulence against *sbm-2* resistance. Virology **355:**52-61.

30. **Johansen IE, Lund OS, Hjulsager CK, Laursen J.** 2001. Recessive resistance in *Pisum sativum* and potyvirus pathotype resolved in a gene-for-cistron correspondence between host and virus. J. Virol. **75:**6609-6614.

31. **Merits A, Guo D, Järvekülg L, Saarma M.** 1999. Biochemical and genetic evidence for interactions between potato A potyvirus-encoded proteins P1 and P3 and proteins of the putative replication complex. Virology **263:**15-22.

32. **Klein PG, Klein RR, Rodríguez-Cerezo E, Hunt AG, Shaw JG.** 1994. Mutational analysis of the tobacco vein mottling virus genome. Virology **204:**759-769.

33. **Suehiro N, Natsuaki T, Watanabe T, Okuda S.** 2004. An important determinant of the ability of *Turnip mosaic virus* to infect *Brassica* spp. and/or *Raphanus sativus* is in its P3 protein. J. Gen. Virol. **85:**2087-2098.

34. **Jenner CE, Wang X, Tomimura K, Ohshima K, Ponz F, Walsh JA.** 2003. The dual role of the potyvirus P3 protein of *Turnip mosaic virus* as a symptom and avirulence determinant in brassicas. Mol. Plant Microbe Interact. **16:**777-784.

35. **Kim BM, Suehiro N, Natsuaki T, Inukai T, Masuta C.** 2010. The P3 protein of *Turnip mosaic virus* can alone induce hypersensitive response-like cell death in *Arabidopsis thaliana* carrying *TuNI*. Mol. Plant Microbe Interact. **23:**144-152.

36. **Cui X, Wei T, Chowda-Reddy RV, Sun G, Wang A.** 2010. The Tobacco etch

virus P3 protein forms mobile inclusions via the early secretory pathway and traffics along actin microfilaments. Virology **397:**56-63.

37. **Lin L, Luo Z, Yan F, Lu Y, Zheng H, Chen J.** 2011. Interaction between potyvirus P3 and ribulose-1,5-bisphosphate carboxylase/oxygenase (RubisCO) of host plants. Virus Genes **43:**90-92.

38. **Shen WT, Wang MQ, Yan P, Gao L, Zhou P.** 2010. Protein interaction matrix of *Papaya ringspot virus* type P based on a yeast two-hybrid system. Acta Virologica **54:**49-54.

39. **Chung BY, Miller WA, Atkins JF, Firth AE.** 2008. An overlapping essential gene in the Potyviridae. Proc. Natl. Acad. Sci. U. S. A. **105:**5897-5902.

40. **Vijayapalani P, Maeshima M, Nagasaki-Takekuchi N, Miller WA.** 2012. Interaction of the trans-frame potyvirus protein P3N-PIPO with host protein PCaP1 facilitates potyvirus movement. PLoS Pathog. **8:**e1002639.

41. **Niehl A, Heinlein M.** 2011. Cellular pathways for viral transport through plasmodesmata. Protoplasma **248:**75-99.

42. **Wei T, Zhang C, Hong J, Xiong R, Kasschau KD, Zhou X, Carrington JC, Wang A.** 2010. Formation of complexes at plasmodesmata for potyvirus intercellular movement is mediated by the viral protein P3N-PIPO. PLoS Pathog. **6:**e1000962.

43. **Ido Y, Nakahara KS, Uyeda I.** 2012. *White clover mosaic virus*-induced gene silencing in pea. J. Gen. Plant Pathol. **78:**127-132.

44. **Sato M, Masuta C, Uyeda I.** 2003. Natural resistance to *Clover yellow vein virus*

720 in beans controlled by a single recessive locus. Mol. Plant Microbe Interact.
721 **16:**994-1002.
722 45. **Takahashi Y, Takahashi T, Uyeda I.** 1997. A cDNA clone to clover yellow vein
723 potyvirus genome is highly infectious. Virus Genes **14:**235-243.
724 46. **Mitsuhara I, Ugaki M, Hirochika H, Ohshima M, Murakami T, Gotoh Y,**
725 **Katayose Y, Nakamura S, Honkura R, Nishimiya S, Ueno K, Mochizuki A,**
726 **Tanimoto H, Tsugawa H, Otsuki Y, Ohashi Y.** 1996. Efficient promoter cassettes
727 for enhanced expression of foreign genes in dicotyledonous and monocotyledonous
728 plants. Plant Cell Physiol. **37:**49-59.
729 47. **Andrade M, Sato M, Uyeda I.** 2007. Two resistance modes to *Clover yellow vein*
730 *virus* in pea characterized by a green fluorescent protein-tagged virus.
731 Phytopathology **97:**544-550.
732 48. **Atsumi G, Nakahara KS, Wada TS, Choi SH, Masuta C, Uyeda I.** 2012.
733 Heterologous expression of viral suppressors of RNA silencing complements
734 virulence of the HC-Pro mutant of clover yellow vein virus in pea. Arch. Virol.
735 **157:**1019-1028.
736 49. **Baranov PV, Gurvich OL, Fayet O, Prère MF, Miller WA, Gesteland RF,**
737 **Atkins JF, Giddings MC.** 2001. RECODE: a database of frameshifting, bypassing
738 and codon redefinition utilized for gene expression. Nucleic Acids Res. **29:**264-267.
739 50. **Nakahara KS, Masuta C, Yamada S, Shimura H, Kashihara Y, Wada TS,**
740 **Meguro A, Goto K, Tadamura K, Sueda K, Sekiguchi T, Shao J, Itchoda N,**
741 **Matsumura T, Igarashi M, Ito K, Carthew RW, Uyeda I.** 2012. Tobacco

742 calmodulin-like protein provides secondary defense by binding to and directing
743 degradation of virus RNA silencing suppressors. Proc. Natl. Acad. Sci. U. S. A.
744 **109:**10113-10118.
745 51. **Menges M, Murray JA.** 2002. Synchronous Arabidopsis suspension cultures for
746 analysis of cell-cycle gene activity. Plant J. **30:**203-212.
747 52. **Komoda K, Naito S, Ishikawa M.** 2004. Replication of plant RNA virus genomes
748 in a cell-free extract of evacuolated plant protoplasts. Proc. Natl. Acad. Sci. USA
749 **101:**1863-1867.
750 53. **Ishibashi K, Komoda K, Ishikawa M.** 2006. In vitro translation and replication of
751 tobamovirus RNA in a cell-free extract of evacuolated tobacco BY-2 protoplasts. In
752 Nagata T, Matsuoka K, Inzé D (eds.), Biotechnology in Agriculture and Forestry.
753 Tobacco BY-2 Cells: From Cellular Dynamics to Omics, Springer, **vol 58:**183-194.
754 54. **Wen RH, Hajimorad MR.** 2010. Mutational analysis of the putative *pipo* of
755 soybean mosaic virus suggests disruption of PIPO protein impedes movement.
756 Virology **400:**1-7.
757 55. **Ratcliff FG, MacFarlane SA, Baulcombe DC.** 1999. Gene silencing without
758 DNA: RNA-mediated cross-protection between viruses. Plant Cell **11:**1207-1215.
759 56. **Chowda-Reddy RV, Sun H, Hill JH, Poysa V, Wang A.** 2011. Simultaneous
760 mutations in multi-viral proteins are required for soybean mosaic virus to gain
761 virulence on soybean genotypes carrying different R genes. PLoS One **6:**e28342.
762 57. **Wei T, Huang TS, McNeil J, Laliberté JF, Hong J, Nelson RS, Wang A.** 2010.
763 Sequential recruitment of the endoplasmic reticulum and chloroplasts for plant

potyvirus replication. J. Virol. **84:**799-809.

58. **Carrington JC, Jensen PE, Schaad MC.** 1998. Genetic evidence for an essential role for potyvirus CI protein in cell-to-cell movement. Plant J. **14:**393-400.

Figure legends

FIG 1 Mapping of the ClYVV genomic region responsible for overcoming *cyv1*-mediated resistance. (A) The diagrams on the left illustrate chimeric constructs based on ClYVV isolate no. 30 (Cl-no30, white) containing nucleotide sequences from 90-1 Br2 (dark gray). The pathogenicity of the chimeric constructs on *cyv1* pea plants was investigated by observing the GFP fluorescence of the uninoculated upper leaves for 37 dpi. Pea cultivar PI 429853 carrying *cyv1* (26) was resistant to Cl-no30. The chimeric viruses designated Cl-BB and RB infected *cyv1* peas systemically, indicating that the P3 cistron of 90-1 BR2 was responsible for breaking the resistance. The figure for PI 429853 indicates the number of infected plants out of the total number of inoculated plants. The infectivity of the constructed chimeric ClYVVs was confirmed by inoculation into susceptible peas (PI 250438). Typical symptoms of PI 250438 leaves infected with the constructed chimeras are shown. (B) Different reactions to Cl-no30 and 90-1 Br2 were observed in a susceptible pea cultivar (PI 250438). The resistance-breaking isolate 90-1 Br2 caused severe dwarfism and mosaic symptoms whereas Cl-no30 caused only vein yellowing and mild mosaic symptoms.

FIG 2 Pea lines that showed resistance to Cl-no30 were inoculated with RB. PI 236493, PI 347420, PI 347422, and PI 429853 carry *cyv1* (26); the other lines were presumed to carry *cyv1* because these lines did not carry *cyv2* and RB broke the resistance of all of the tested pea lines around 5 wpi. R, resistant to the inoculated virus; S, susceptible to the inoculated virus.

FIG 3 Comparison of the nucleotide and amino acid sequences encoded by the P3 cistrons in avirulent (Cl-no30) and resistance-breaking (90-1 Br2) isolates. (A) Alignment of the nucleotide sequences of P3 from Cl-no30 and 90-1 Br2. 90-1 Br2 possesses 58 nucleotide differences, including synonymous differences, compared with Cl-no30 in the mapped P3 region (underlined in gray). Yellow boxes indicate non-synonymous differences with respect to the P3 amino acid sequences but synonymous with respect to the PIPO amino acid sequences. Orange boxes indicate non-synonymous differences with respect to the PIPO amino acid sequences but synonymous with respect to the P3 amino acid sequences. The black triangle indicates the position of a non-synonymous difference at position 38 in the PIPO amino acid sequences among ClYVV isolates (see also [C]). Asterisk 1 corresponds to the end of PIPO in Cl-no30 and to position 62 in the 90-1 Br2 PIPO amino acid sequence. Asterisk 2 corresponds to the end of PIPO from 90-1 Br2. RB possesses the genomic sequence of the 90-1 Br2 P3 cistron upstream of the *Bgl*II site (underlined in gray). (B) Alignment of the P3 amino acid sequences from Cl-no30 and 90-1 Br2. The black triangle, asterisks 1 and 2, and gray underlining are shown in the positions corresponding to

808 those in (A). (C) Comparison of the PIPO amino acid sequences from ClYVV isolate
809 Cl-no30, which was avirulent to *cyv1* pea, and others that sometimes broke *cyv1* resistance.
810 Compared with Cl-no30, the *cyv1* resistance-breaking isolates possessed two differences in
811 amino acid sequence: a change from T to I at position 38 (black triangle) and an addition of
812 9 to 15 amino acids beginning at position 62 (asterisk 1). ClYVV isolates 90-1 Br2, N
813 (accession number AB732964), I89-1 (AB732963), and MB3 (AB732965) induced
814 necrosis or mosaic symptoms in *cyv1* pea when they broke *cyv1* resistance (data not shown).
815 Asterisk 2 is shown at the position corresponding to that in (A) (i.e., the end of 90-1 Br2
816 PIPO).
817
818 **FIG 4** Genetic analysis of the roles of P3 and P3N-PIPO in the breaking of *cyv1* resistance.
819 (A) Examination of the role of P3N-PIPO. Nucleotide differences were introduced into the
820 P3 cistrons of Cl-no30 and RB that caused differences in the PIPO amino acid sequence at
821 amino acids 38 and 62, but did not affect the sequence of P3. P3N-PIPO of Cl-no30 is 15
822 amino acid residues shorter than that of RB. Substitutions at one or both positions were
823 introduced into Cl-no30 and RB infectious clones, which were then inoculated into *cyv1*
824 peas. The substitution at position 62 of Cl-no30 [TAA (stop codon) → CAA (glutamine) in
825 constructs Cl/PIPO$^{T38I, 62Q}$ and Cl/PIPO^{62Q}] resulted in four differences in the amino acid
826 sequence of P3N-PIPO (black lines) compared with that of RB. The pathogenicity of these
827 clones was monitored by GFP fluorescence and either RT-PCR or RT-nested PCR (results
828 marked with "[a]"), which amplified the cDNA sequence of ClYVV NIb in RNA extracts
829 from the upper leaves of inoculated plants at 35 dpi. (B) Examination of the role of P3 in

the breaking of *cyv1* resistance in pea. In RB/P3^{KII}PIPO^{62Q}, the PIPO coding region and upstream region of RB P3 were exchanged with the corresponding region of Cl-no30. In Cl/P3^{RAM}, a region downstream of PIPO of Cl-no30 was replaced with the corresponding sequence from RB. The pathogenicity of the ClYVV mutants was checked as in (A). (C) Role of the N-terminal sequence of P3 in the breaking of *cyv1* resistance. Isolate 90-1, from which 90-1 Br2 originated, is avirulent to pea carrying *cyv1* and possesses arginine (R) at position 28 in the N-terminal region of P3; isolate 90-1 Br2, which is virulent to *cyv1* pea, has methionine (M) at this position. Cl-no30 contains lysine (K) at position 28. Nucleotide substitutions were introduced at this position in Cl-no30 and RB and designated as Cl/P3&P3N-PIPO^{K28M}, RB/P3&P3N-PIPO^{M28K}, and RB/P3&P3N-PIPO^{M28R}, each containing the indicated substitution. These mutants were independently inoculated onto *cyv1* and their virulence was examined as in (A). Black bars indicate the amino acid substitution at position 28 in the N-terminus of P3. NT: not tested. When the Cl-no30 and RB point mutants used in Fig. 4 were inoculated into a susceptible pea line (PI 250438), they infected the uninoculated upper leaves at 1 wpi, indicating their similar infectivity in a susceptible pea line.

FIG 5 Effect of the additional production of P3 and P3N-PIPO in *cis* and *trans* on the cell-to-cell movement of Cl-no30 in *cyv*1 pea. (A) Cl-no30 and pE2113 vectors designed to produce P3 and P3N-PIPO from Cl-no30 and RB were co-bombarded onto PI 429853. The cell-to-cell movement of Cl-no30 was monitored by observing GFP fluorescence at 3 days post-bombardment. Constructs with names ending in P3 were expected to produce the P3

852 protein plus a small amount of P3N-PIPO. Constructs with names ending in P3N-PIPO and
853 P3ΔPIPO produced P3N-PIPO and P3, respectively, exclusively. (B) The P3 cistrons that
854 produced P3 (Cl/P3ΔPIPO) or P3N-PIPO (Cl/P3N-PIPO) exclusively were inserted
855 between P1 and HC-pro of Cl-no30 and bombarded onto detached leaves of pea carrying
856 *cyv1* (PI 429853). GFP fluorescence was monitored at 3 days post-bombardment.
857
858 **FIG 6** P3N-PIPO accumulated to higher levels in a susceptible pea line (PI 250438)
859 infected with RB than in those infected with Cl-no30. (A) Western blot analysis of P3
860 (upper panel) and P3N-PIPO (middle panel), which migrated at around 40 and 24 kDa,
861 respectively, was conducted with samples from the upper leaves of peas infected with
862 Cl-no30 and RB. Samples were taken at 9 dpi. The band considered to be P3N-PIPO was
863 only detected in samples from RB-infected peas (arrowheads). Asterisks indicate
864 non-specific signals. The gel stained with Coomassie Brilliant Blue (CBB) is shown as a
865 loading control (lower panel). Similar results were obtained in independent experiments
866 (Experiments 1 and 2). (B) Confirmation of antibodies raised against PIPO. The expression
867 of GST-fused PIPO (GST-PIPO) was induced with 0.1 mM IPTG (see Materials and
868 Methods). Lanes 1 and 2 are samples from *E. coli* transformants that contained the cDNA
869 expressing PIPO fused with GST. Lane C is from a sample transformed with the vector
870 expressing the S8 protein of rice ragged stunt virus fused with GST as a control. The
871 asterisk indicates a non-specific band (loading control). (C) *In vitro* analysis of P3N-PIPO
872 production. RNAs were translated in the presence of [^{35}S]methionine. The translation
873 products were separated by 4–12% SDS-PAGE, and the signals were visualized by

874 autoradiography. The positions of P3 and P3N-PIPO are shown to the right of the panel.
875 Arrowheads indicate the bands corresponding to RB P3N-PIPO. Molecular mass markers
876 (kDa) are indicated to the left of the panel.
877
878 **FIG 7** Higher levels of P3N-PIPO contribute to the breaking of *cyv1* resistance.
879 Co-inoculation with Cl-no30 and WClMV producing P3N-PIPO from Cl-no30
880 (WCl/no30_P3N-PIPO) or RB (WCl/RB_P3N-PIPO) enabled systemic infection with
881 Cl-no30. The systemic infection of *cyv1* peas (PI 429853) with ClYVV (upper panel) and
882 WClMV (middle panel) was detected in samples from uninoculated upper leaves by
883 RT-PCR for WClMV CP and RT-nested PCR for ClYVV NIb. Stability of the transgene
884 P3N-PIPO in the WClMV vectors was confirmed by RT-PCR with primers corresponding
885 to the upstream region of the WClMV multi-cloning site and 3′-terminus of the PIPO open
886 reading frame (lower panel) at 11 dpi. The tests were run in duplicate with three *cyv1* pea
887 plants (PI 429853, written as PI42-1, -2, and -3) per co-inoculation test. Essentially similar
888 results were obtained, and one set is shown. PI250: PI 250438, a cultivar susceptible to both
889 ClYVV and WClMV. M: 100-bp DNA ladder marker. Mock: a pea plant (PI 250438)
890 inoculated with 0.01 M phosphate buffer.
891
892

893 **TABLE 1** Cell-to-cell movement of ClYVV with point mutants in P3N-PIPO in *cyv1* pea

894 PI 429853 at 5 dpi. All mutants are illustrated in Fig. 4A and Fig 5B.

Mutant	Moving[a]	Restricted to single cell[b]	Total number of examined infected cells	Cell-to-cell movement rate[c] (%)
Cl-no30	2	40	42	5
Cl/PIPO^{62Q}	15	27	42	36
RB	15	23	38	39
RB/PIPO^{I38T}	5	79	84	6
RB/PIPO^{Q62}	11	33	44	25
Cl/P3ΔPIPO	2	14	16	12
Cl/P3N-PIPO	12	38	50	24

895 a Number of foci where mutants spread to two or more surrounding cells from the initially

896 infected single cells.

897 b Number of foci where mutants were restricted to the initially infected single cell.

898 c The percentage of foci where mutants moved to neighboring cells, calculated as [(number

899 of foci where mutants moved to neighboring cells) / (total number of foci)] × 100.

900

TABLE 2 The effect of transiently expressed P3N-PIPO on movement of Cl-no30 in *cyv1* pea (PI 429853) at 5 dpi.

Cl-no30 +	PI 250438[a]			PI 429853		
	Single cell[b]	Moving [c]	Cell-to-cell movement rate[d] (%)	Single cell[b]	Moving [c]	Cell-to-cell movement rate[d] (%)
Empty[e]	9	22	71	40	2	4.7
pE2113/no30_P3	2	77	97	75	3	3.8
pE2113/no30_P3N-PIPO	8	79	91	102	33	32.4
pE2113/no30_P3ΔPIPO	8	81	91	90	7	7.2
pE2113/RB_P3	5	140	97	83	11	13.3
pE2113/RB_P3N-PIPO	3	110	97	145	41	28.3
pE113/RB_P3ΔPIPO	2	12	86	39	4	10.3

a Each co-bombardment test was simultaneously carried out with susceptible pea, PI 250438, as a positive control.

b The number of foci where Cl-no30 was restricted to the initially infected single cell.

c The number of foci where Cl-no30 moved to two or more cells.

d The percentage of foci where Cl-no30 moved to neighboring cells, calculated as (number of foci where Cl-no30 moved to neighboring cells) / (total number of foci) × 100.

e Only Cl-no30 was bombarded into the plants.

FIG. 1

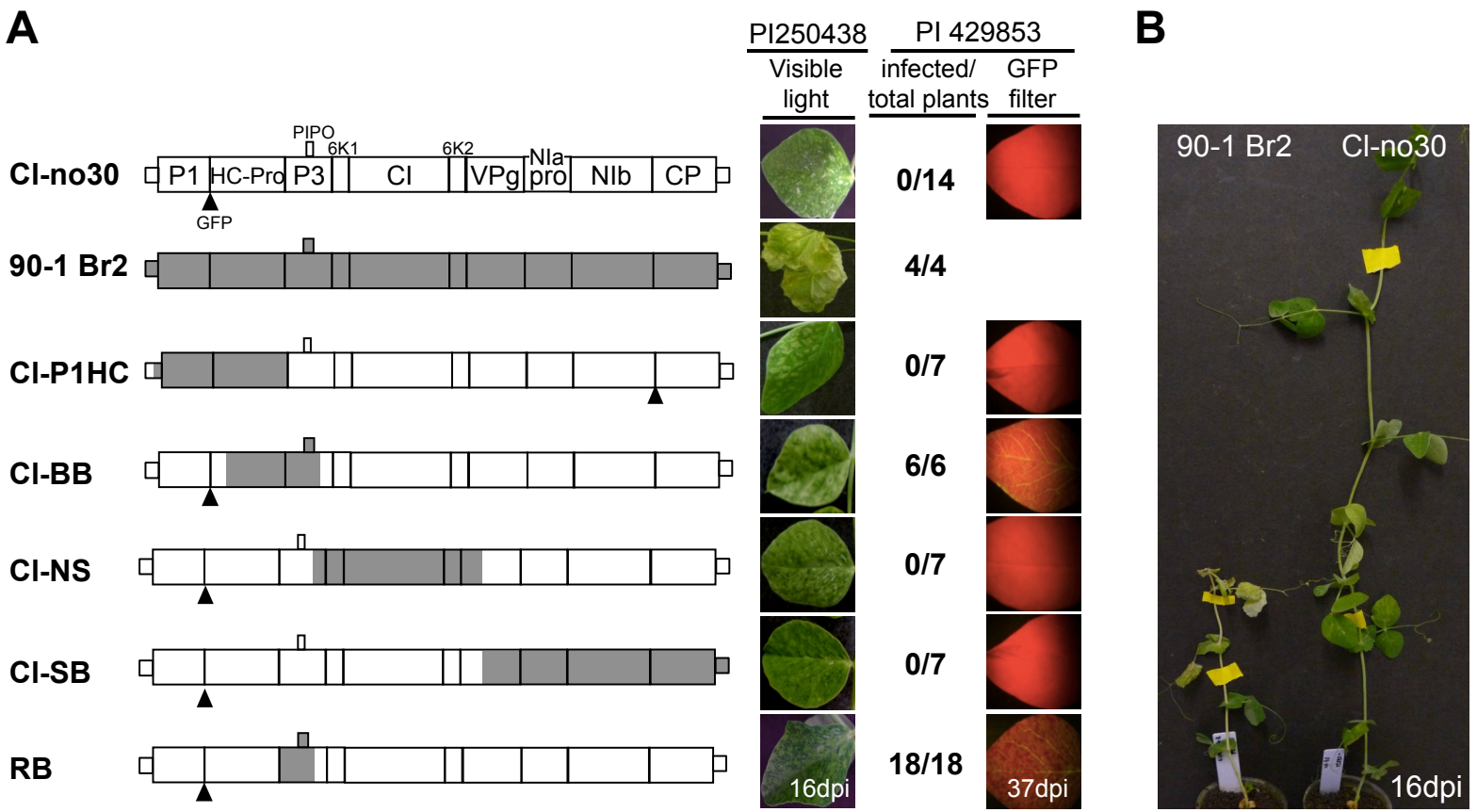
A
PI250438
PI 429853
Visible light
infected/ total plants
GFP filter
PIPO
6K1
6K2
NIa-pro
P1
HC-Pro
P3
CI
VPg
NIb
CP
GFP
CI-no30
90-1 Br2
CI-P1HC
CI-BB
CI-NS
CI-SB
RB
0/14
4/4
0/7
6/6
0/7
0/7
18/18
16dpi
37dpi
B
90-1 Br2
CI-no30
16dpi

FIG. 2

Pea line	Inoculated plants: Cl-no30 Infection profiles	Inoculated plants: RB Infection profiles	Inoculated plants: RB GFP filter
PI 236493	R	S	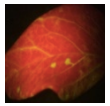
PI 347420	R	S	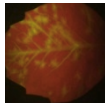
PI 347422	R	S	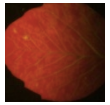
PI 429853	R	S	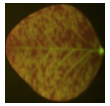
PI 347295 RS-7	R	S	
PI 347295 R-18	R	S	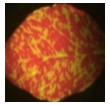
PI 116843 R-8	R	S	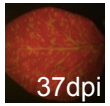

FIG. 3

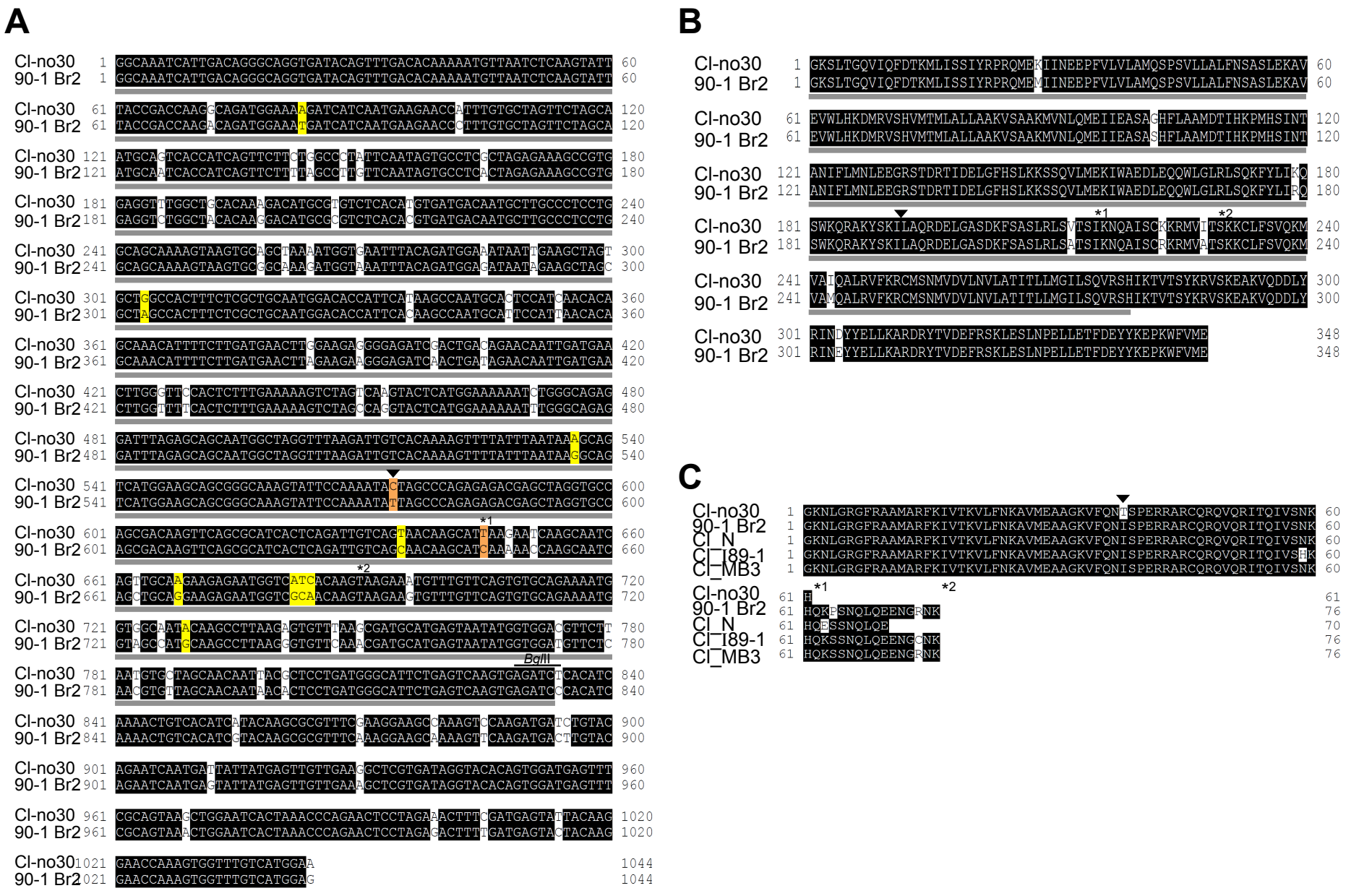
A
Cl-no30 1 GGCAAATCATTGACAGGGCAGGTGATACAGTTTGACACAAAAATGTTAATCTCAAGTATT 60
90-1 Br2 1 GGCAAATCATTGACAGGGCAGGTGATACAGTTTGACACAAAAATGTTAATCTCAAGTATT 60
Cl-no30 61 TACCGACCAAGGCAGATGGAAAAGATCATCAATGAAGAACCATTTGTGCTAGTTCTAGCA 120
90-1 Br2 61 TACCGACCAAGACAGATGGAAATGATCATCAATGAAGAACCCTTTGTGCTAGTTCTAGCA 120
Cl-no30 121 ATGCAGTCACCATCAGTTCTTCTGGCCCTATTCAATAGTGCCTCGCTAGAGAAAGCCGTG 180
90-1 Br2 121 ATGCAATCACCATCAGTTCTTTTAGCCTTGTTCAATAGTGCCTCACTAGAGAAAGCCGTG 180
Cl-no30 181 GAGGTTTGGCTGCACAAAGACATGCGTGTCTCACATGTGATGACAATGCTTGCCCTCCTG 240
90-1 Br2 181 GAGGTCTGGCTACACAAGGACATGCGCGTCTCACACGTGATGACAATGCTTGCCCTCCTG 240
Cl-no30 241 GCAGCAAAAGTAAGTGCAGCTAAAATGGTGAATTTACAGATGGAATAATTGAAGCTAGT 300
90-1 Br2 241 GCAGCAAAAGTAAGTGCGGCAAAGATGGTAAATTTACAGATGGAGATAATAGAAGCTAGC 300
Cl-no30 301 GCTGGCCACTTTCTCGCTGCAATGGACACCATTCATAAGCCAATGCACTCCATCAACACA 360
90-1 Br2 301 GCTAGCCACTTTCTCGCTGCAATGGACACCATTCACAAGCCAATGCATTCCATTAACACA 360
Cl-no30 361 GCAAACATTTTCTTGATGAACTTGGAAGAGGGGAGATCGACTGAGAGAACAATTGATGAA 420
90-1 Br2 361 GCAAACATTTTCTTGATGAACTTAGAAGAAGGGAGATCAACTGATAGAACAATTGATGAA 420
Cl-no30 421 CTTGGGTTCCACTCTTTGAAAAAGTCTAGTCAAGTACTCATGGAAAAAATCTGGGCAGAG 480
90-1 Br2 421 CTTGGTTTTCACTCTTTGAAAAAGTCTAGCCAGGTACTCATGGAAAAAATTTGGGCAGAG 480
Cl-no30 481 GATTTAGAGCAGCAATGGCTAGGTTTAAGATTGTCACAAAAGTTTTATTTAATAAAGCAG 540
90-1 Br2 481 GATTTAGAGCAGCAATGGCTAGGTTTAAGATTGTCACAAAAGTTTTATTTAATAAGGCAG 540
Cl-no30 541 TCATGGAAGCAGCGGGCAAAGTATTCCAAAATAGTAGCCCAGAGAGACGAGCTAGGTGCC 600
90-1 Br2 541 TCATGGAAGCAGCGGGCAAAGTATTCCAAAATATTAGCCCAGAGAGACGAGCTAGGTGCC 600
*1
Cl-no30 601 AGCGACAAGTTCAGCGCATCACTCAGATTGTCAGTAACAAGCATTAAGAATCAAGCAATC 660
90-1 Br2 601 AGCGACAAGTTCAGCGCATCACTCAGATTGTCAGCAACAAGCATGAAAAACAAGCAATC 660
*2
Cl-no30 661 AGTTGCAAGAAGAGAATGGTCATCACAAGTAAGAAAATGTTTGTTCAGTGTGCAGAAAATG 720
90-1 Br2 661 AGCTGCAGGAAGAGAATGGTCGCAACAAGTAAGAAGTGTTTGTTCAGTGTGCAGAAAATG 720
Cl-no30 721 GTGGCAATACAAGCCTTAAGAGTGTTTAAGCGATGCATGAGTAATATGGTGGACGTTCTT 780
90-1 Br2 721 GTAGCCATGCAAGCCTTAAGGGTGTTCAAACGATGCATGAGTAATATGGTGGATGTTCTC 780
BglII
Cl-no30 781 AATGTGCTAGCAACAATTACGCTCCTGATGGGCATTCTGAGTCAAGTGAGATCTCACATC 840
90-1 Br2 781 AACGTGTTAGCAACAATTACACTCCTGATGGGCATTCTGAGTCAAGTGAGATCCCACATC 840
Cl-no30 841 AAAACTGTCACATCATACAAGCGCGTTTCGAAGGAAGCCAAAGTCCAAGATGATCTGTAC 900
90-1 Br2 841 AAAACTGTCACATCGTACAAGCGCGTTTCAAAGGAAGCAAAAGTTCAAGATGACTTGTAC 900
Cl-no30 901 AGAATCAATGATTATTATGAGTTGTTGAAGGCTCGTGATAGGTACACAGTGGATGAGTTT 960
90-1 Br2 901 AGAATCAATGAGTATTATGAGTTGTTGAAAGCTCGTGATAGGTACACAGTGGATGAGTTT 960
Cl-no30 961 CGCAGTAAGCTGGAATCACTAAACCCAGAACTCCTAGAAACTTTCGATGAGTATTACAAG 1020
90-1 Br2 961 CGCAGTAAACTGGAATCACTAAACCCAGAACTCCTAGAGACTTTTGATGAGTACTACAAG 1020
Cl-no30 1021 GAACCAAAGTGGTTTGTCATGGAA 1044
90-1 Br2 1021 GAACCAAAGTGGTTTGTCATGGAG 1044
B
Cl-no30 1 GKSLTGQVIQFDTKMLISSIYRPRQMEKIINEEPFVLVLAMQSPSVLLALFNSASLEKAV 60
90-1 Br2 1 GKSLTGQVIQFDTKMLISSIYRPRQMEMIINEEPFVLVLAMQSPSVLLALFNSASLEKAV 60
Cl-no30 61 EVWLHKDMRVSHVMTMLALLAAKVSAAKMVNLQMEIIEASAGHFLAAMDTIHKPMHSINT 120
90-1 Br2 61 EVWLHKDMRVSHVMTMLALLAAKVSAAKMVNLQMEIIEASASHFLAAMDTIHKPMHSINT 120
Cl-no30 121 ANIFLMNLEEGRSTDRTIDELGFHSLKKSSQVLMEKIWAEDLEQQWLGLRLSQKFYLIKQ 180
90-1 Br2 121 ANIFLMNLEEGRSTDRTIDELGFHSLKKSSQVLMEKIWAEDLEQQWLGLRLSQKFYLIRQ 180
*1
*2
Cl-no30 181 SWKQRAKYSKILAQRDELGASDKFSASLRLSWTSIKNQAISCKKRMVITSKKCLFSVQKM 240
90-1 Br2 181 SWKQRAKYSKILAQRDELGASDKFSASLRLSATSIKNQAISCPKRMVATSKKCLFSVQKM 240
Cl-no30 241 VAIQALRVFKRCMSNMVDVLNVLATITLLMGILSQVRSHIKTVTSYKRVSKEAKVQDDLY 300
90-1 Br2 241 VAMQALRVFKRCMSNMVDVLNVLATITLLMGILSQVRSHIKTVTSYKRVSKEAKVQDDLY 300
Cl-no30 301 RINDYYELLKARDRYTVDEFRSKLESLNPELLETFDEYYKEPKWFVME 348
90-1 Br2 301 RINEYYELLKARDRYTVDEFRSKLESLNPELLETFDEYYKEPKWFVME 348
C
Cl-no30 1 GKNLGRGFRAAMARFKIVTKVLFNKAVMEAAGKVFQNTSPERRARCQRQVQRITQIVSNK 60
90-1 Br2 1 GKNLGRGFRAAMARFKIVTKVLFNKAVMEAAGKVFQNISPERRARCQRQVQRITQIVSNK 60
Cl_N 1 GKNLGRGFRAAMARFKIVTKVLFNKAVMEAAGKVFQNISPERRARCQRQVQRITQIVSNK 60
Cl_I89-1 1 GKNLGRGFRAAMARFKIVTKVLFNKAVMEAAGKVFQNISPERRARCQRQVQRITQIVSHK 60
Cl_MB3 1 GKNLGRGFRAAMARFKIVTKVLFNKAVMEAAGKVFQNISPERRARCQRQVQRITQIVSNK 60
*1
*2
Cl-no30 61 H 61
90-1 Br2 61 HQKPSNQLQEENGRNK 76
Cl_N 61 HQESSNQLQE 70
Cl_I89-1 61 HQKSSNQLQEENGQNK 76
Cl_MB3 61 HQKSSNQLQEENGRNK 76

FIG. 4

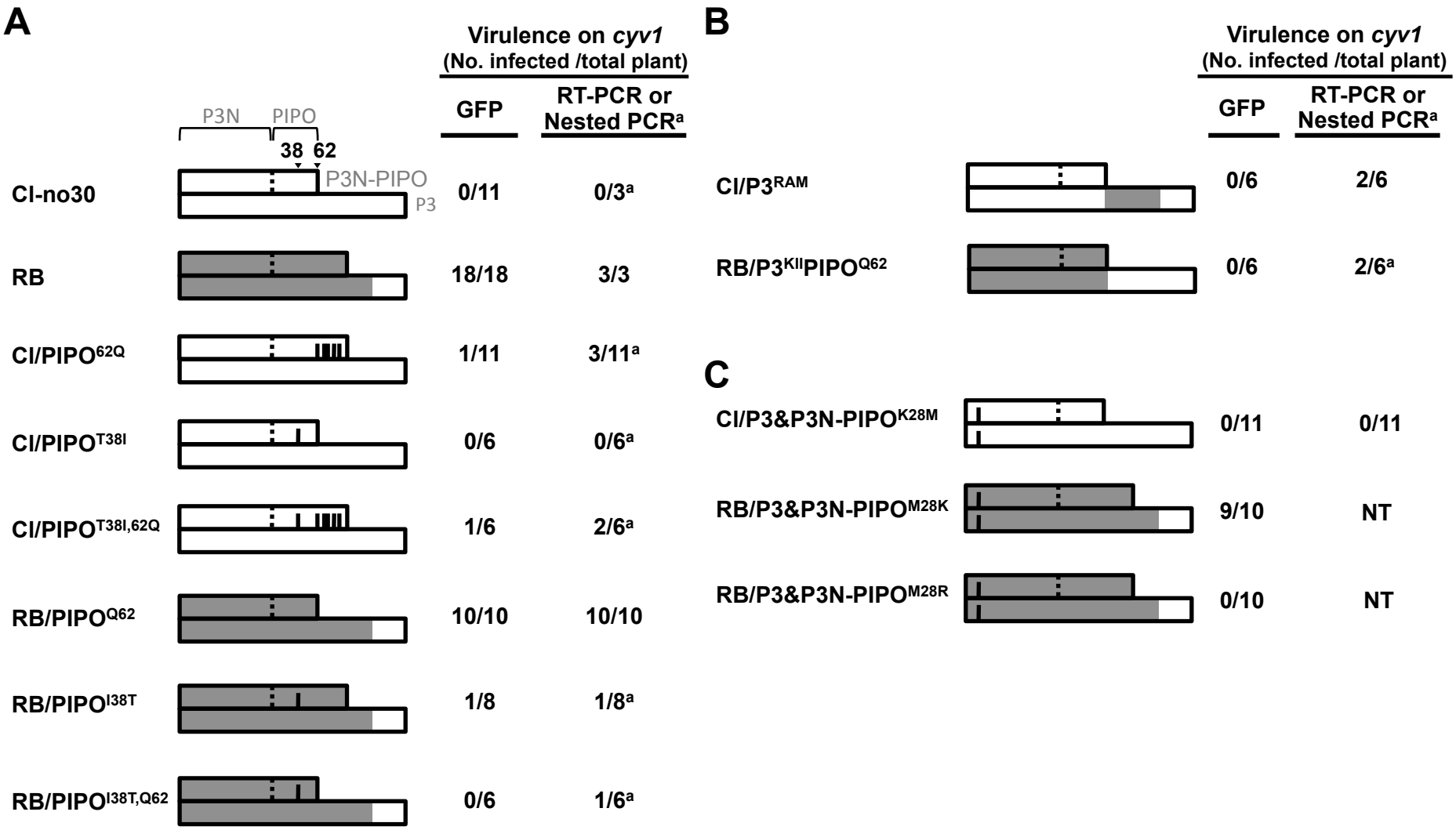
A
Virulence on cyv1 (No. infected /total plant)
GFP
RT-PCR or Nested PCR[a]
P3N
PIPO
38
62
P3N-PIPO
P3
Cl-no30
0/11
0/3[a]
RB
18/18
3/3
Cl/PIPO62Q
1/11
3/11[a]
Cl/PIPOT38I
0/6
0/6[a]
Cl/PIPOT38I,62Q
1/6
2/6[a]
RB/PIPOQ62
10/10
10/10
RB/PIPOI38T
1/8
1/8[a]
RB/PIPOI38T,Q62
0/6
1/6[a]
B
Virulence on cyv1 (No. infected /total plant)
GFP
RT-PCR or Nested PCR[a]
Cl/P3RAM
0/6
2/6
RB/P3KIIPIPOQ62
0/6
2/6[a]
C
Cl/P3&P3N-PIPOK28M
0/11
0/11
RB/P3&P3N-PIPOM28K
9/10
NT
RB/P3&P3N-PIPOM28R
0/10
NT

FIG. 5

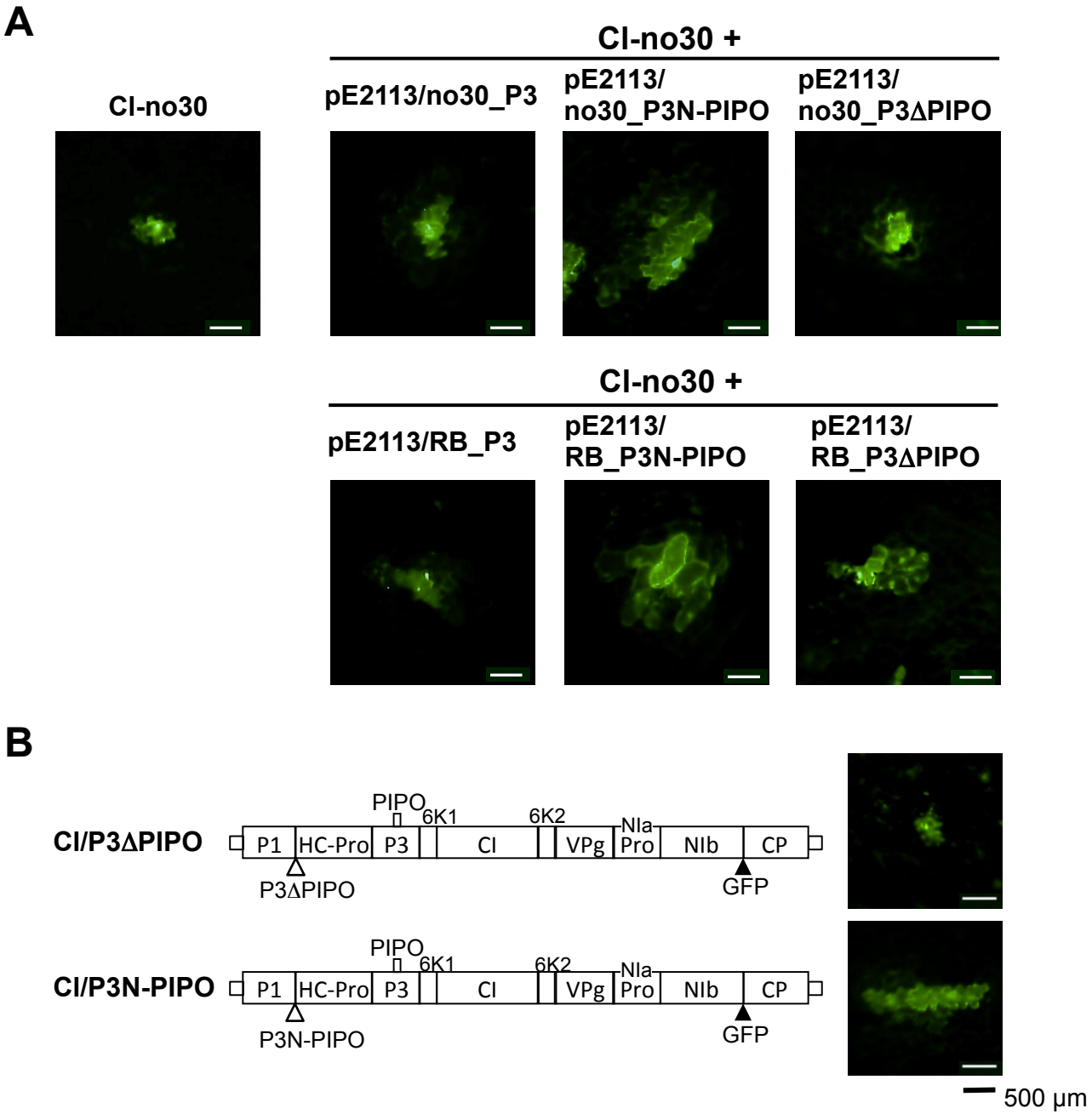
A
CI-no30 +
CI-no30
pE2113/no30_P3
pE2113/ no30_P3N-PIPO
pE2113/ no30_P3ΔPIPO
CI-no30 +
pE2113/RB_P3
pE2113/ RB_P3N-PIPO
pE2113/ RB_P3ΔPIPO
B
CI/P3ΔPIPO
PIPO
6K1
6K2
NIa
P1
HC-Pro
P3
CI
VPg
Pro
NIb
CP
P3ΔPIPO
GFP
CI/P3N-PIPO
P3N-PIPO
500 μm

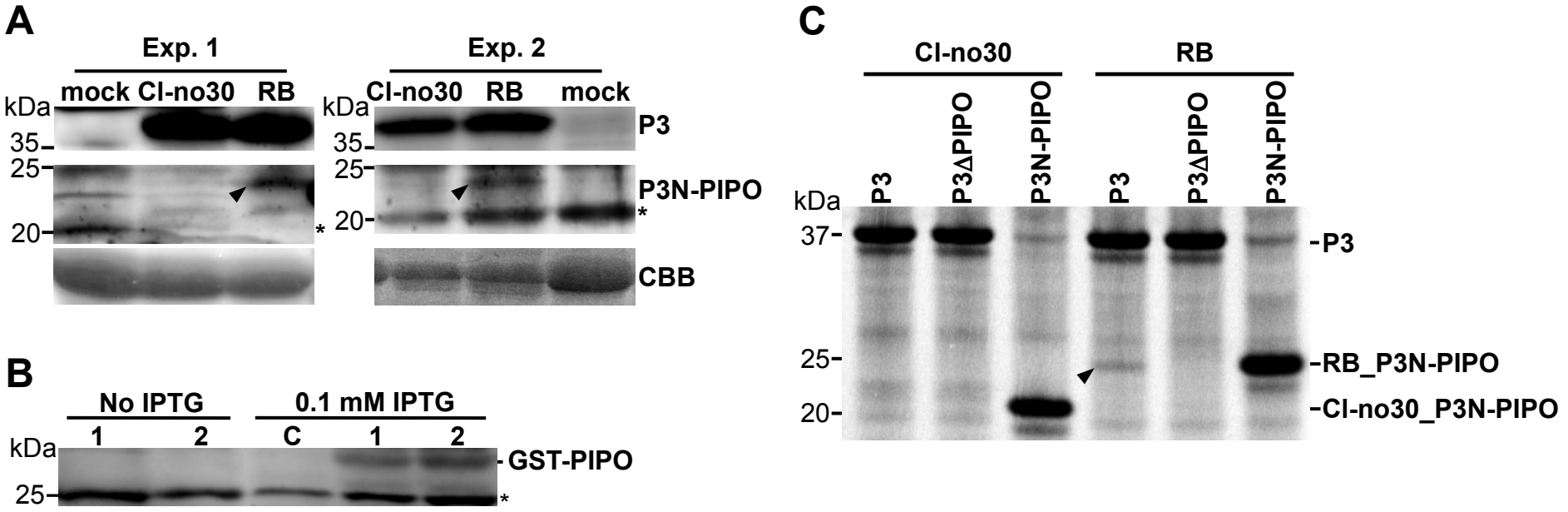
A
Exp. 1
mock
Cl-no30
RB
kDa
35
25
20
Exp. 2
Cl-no30
RB
mock
P3
P3N-PIPO
CBB
B
No IPTG
0.1 mM IPTG
1
2
C
1
2
kDa
25
GST-PIPO
C
Cl-no30
RB
P3
P3ΔPIPO
P3N-PIPO
kDa
37
25
20
P3
RB_P3N-PIPO
Cl-no30_P3N-PIPO

FIG. 7

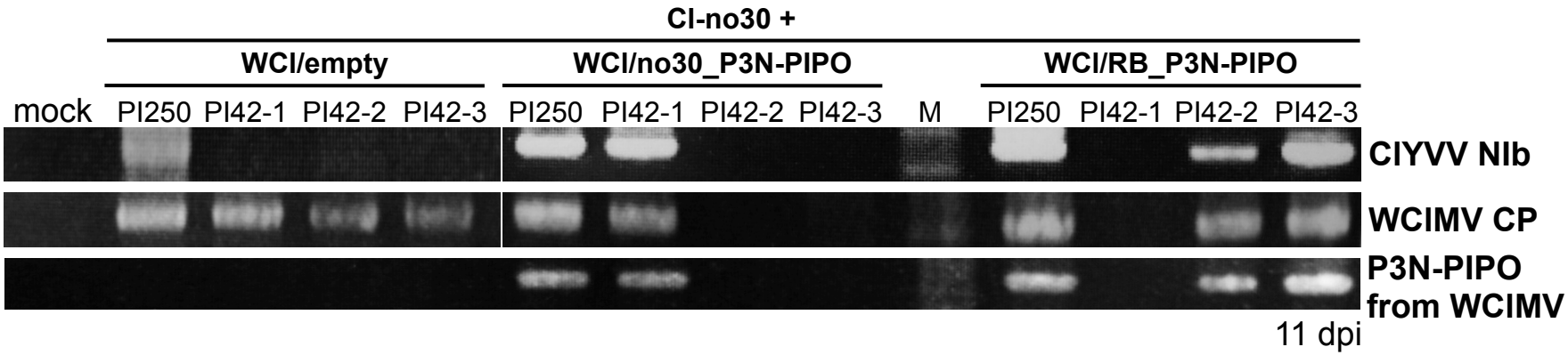
Cl-no30 +
WCl/empty
WCl/no30_P3N-PIPO
WCl/RB_P3N-PIPO
mock
PI250
PI42-1
PI42-2
PI42-3
PI250
PI42-1
PI42-2
PI42-3
M
PI250
PI42-1
PI42-2
PI42-3
ClYVV NIb
WCIMV CP
P3N-PIPO from WCIMV
11 dpi